

SOLAR POWER UNMANNED AERIAL VEHICLE: HIGH ALTITUDE LONG
ENDURANCE APPLICATIONS (HALE-SPUAV)

A project

Presented to

The Faculty of the Department of Mechanical and Aerospace Engineering

San Jose State University

In Partial Fulfillment

Of the Requirements for the Degree

Master of Science

By

Manish R. Bhatt

May 2012

© 2012

Manish R. Bhatt

ALL RIGHTS RESERVED

The Designated Committee Approves the Project Titled

SOLAR POWER UNMANNED AERIAL VEHICLE: HIGH ALTITUDE LONG
ENDURANCE APPLICATIONS (HALE-SPUAV)

By

MANISH R. BHATT

APPROVED FOR THE DEPARTMENT OF MECHANICAL AND AEROSPACE
ENGINEERING

SAN JOSE STATE UNIVERSITY

May 2012

Dr. Nikos Mourtos Committee Chair, San Jose State University

Dr. Periklis Papadopoulos Committee member, San Jose State University

Kanu Vyas Committee member, Boeing Commercial Airplanes

ABSTRACT

SOLAR POWER UNMANNED AERIAL VEHICLE: HIGH ALTITUDE LONG ENDURANCE APPLICATIONS (HALE-SPUAV)

By Manish R Bhatt

This project deals with UAV using solar energy as their only source of energy for more than 24 hours flight. Using solar panels, it collects the energy during the day for immediate use but also store the remaining part for the night flight. The objective is to identify, design and analyze such a reusable solar power unmanned areal vehicle for high altitude long endurance application with successful implementation of higher energy density batteries such as Li-su.

A detail analysis has been performed to compare similar airplanes to study their successes and failure. An aircraft with similar wingspan as NASA Helios and remarkably less weight, nearly 1135lb, than it is been design. A weight analysis and power sensitivity analysis were researched, and it was shown that this aircraft would generate 75kw of power that is greater then the power available to fly.

ACKNOWLEDGEMENTS

This project could never have been completed without the endless support of my committee members, friends and family.

First, I would like to thank Professor Nikos Mourtos for his technical guidance and knowledge of aircraft design. During the time of my masters he has provided me an endless support personally and technically. Without him not even this report also my graduate studies would not have been possible.

Second, I wish to thank Professor Perklis Papadopoulos for his opinions and recommendations. Throughout my research, he has provided me help whenever needed and broadened my knowledge and expertise in the field of CFD.

Third, I would like to thank Kanu Vyas for taking time to tech me in our chaotic work environment throughout this study.

Finally, I would like to thank my family and my close friends for being there, without your encouragement I would not be where I am today.

TABLE OF CONTENTS

LIST OF FIGURES.....	X
LIST OF TABLES.....	XII
1.0 INTRODUCTION.....	1
1.1 MOTIVATION.....	1
1.2 OBJECTIVE.....	2
1.3 LITERATURE REVIEW.....	2
1.3.1 UAV.....	3
1.3.2 UAV HISTORY AND TIMELINE.....	3
1.3.3 CLASSIFICATION OF UAVs.....	6
1.4 SOLAR FLIGHT.....	9
2.0 MISSION SPECIFICATION.....	13
2.1 MISSION PROFILE.....	13
2.2 MARKET ANALYSIS.....	14
2.3 TECHNICAL AND ECONOMICAL FEASIBILITY.....	15
2.4 CRITICAL MISSION REQUIREMENTS.....	15
3.0 COMPARATIVE STUDY OF SIMILAR AIRPLANES.....	15
3.1 MISSION CAPABILITIES AND CONFIGURATION SELECTION.....	15
3.2 COMPARISON OF IMPORTANT DESIGN PARAMETERS.....	16
4.0 COMPARATIVE STUDY OF THE AIRPLANE WITH THE SIMILAR MISSION PERFORMANC.....	17
5.0 SELECTION OF PROPULSION SYSTEM.....	18
5.1 SELECTION OF NUMBER OF ENGINES.....	18

5.2	PROPELLER SIZING.....	18
6.0	CONFIGURATION SELECTION.....	19
6.0	OVERALL CONFIGURATION.....	19
6.1	WING CONFIGURATION.....	19
6.2	EMPENNAGE CONFIGURATION.....	23
6.3	LANDING GEAR DISPOSITION.....	23
6.4	PROPOSED CONFIGURATION.....	23
7.0	MISSION WEIGHT ESTIMATES.....	24
7.1	COMMENTS.....	24
7.2	SOLAR SYSTEM WEIGHTS.....	24
7.3	AIRFRAME WEIGHT.....	26
8.0	PERFORMANCE CONSTRAINT ANALYSIS.....	27
8.1	COMMENTS.....	27
8.2	SIZING TO CRUISE SPEED.....	28
8.3	SIZING TO FAR23 RATE OF CLIMB REQUIREMENTS.....	29
8.4	PERFORMANCE SIZING CALCULATION.....	29
8.5	POWER REQUIREMENT ANALYSIS.....	30
9.0	FUSELAGE DESIGN.....	32
10.0	LANDING GEAR DESIGN.....	32
11.0	WING, HIGH LIFT SYSTEM, AND LATERAL CONTROLS DESIGN.....	33
11.1	WING PLANFORM DESIGN.....	33
11.2	TAPER RATIO.....	33
11.3	DIHEDRAL ANGLE.....	34

11.4	INCIDENCE ANGLE.....	34
11.5	CONTROL SURFACES.....	34
11.6	WING CAD DRAWING.....	36
12.0	EMPENNAGE AND CONTROL ANALYSIS.....	37
12.1	OVERALL EMPENNAGE DESIGN.....	36
12.2	EMPENNAGE AIRFOIL.....	36
12.3	DESIGN OF THE LONGITUDINAL AND DIRECTIONAL CONTROLS...	40
13.0	WEIGHT AND BALANCE.....	40
13.1	COMPONENT WEIGHT BREAKDOWN.....	40
13.1.1	MAXIMUM POWER POINT TRACKER.....	40
13.1.2	AVIONICS.....	42
13.1.3	MOTORS.....	42
13.2	CENTER OF GRAVITY CALCULATION.....	44
14.0	STABILITY ANALYSIS.....	45
15.0	DRAG POLAR ESTIMATION.....	50
15.1	AIRPLANE ZERO LIFT DRAG.....	50
15.2	AIRPLANE DRAG POLAR.....	51
15.3	DISCUSSION.....	52
16.0	ENVIRONMENTAL/ECONOMICAL TRADEOFFS.....	52
16.1	ENVIRONMENTAL CONSIDERATION.....	52
16.2	ECONOMIC FEASIBILITY.....	53
17.0	CONCLUSION/RECOMMENDATION.....	54
	REFERENCE.....	55

APPENDICES.....	56
APPENDIX A: COMPLETE DESIGN PARAMETERS FOR SIMILAR AIRCRAFT.....	57
APPENDIX B: LANDING GEAR POSITIONS.....	59
APPENDIX C & E: WING & AIRCRAFT CAD DRAWINGS.....	59
Appendix D: EMPENNAGE CAD DRAWINGS.....	61
APPENDIX F: XFLR5 DATA.....	61

LIST OF FIGURES

Figure 1: NASA-funded Gossamer Penguin by AeroVironment.....	9
Figure 2: NASA Pathfinder Plus.....	10
Figure 3: NASA Centurion.....	11
Figure 4: NASA Helios.....	12
Figure 5: Mission Profile for HALE-SPUAV.....	14
Figure 6: Selig 1223 Airfoil with Unit Length.....	20
Figure 7: XFLR5 Reynolds Number Legend (0.050 is 50000, 0.1 is 100,000, etc.).....	21
Figure 8: Lift-to-Drag Ratio as a Function of Angle of Attack.....	21
Figure 9: Lift Coefficient as a Function of Angle of Attack.....	21
Figure 10: Lift Coefficient as a Function of Drag Coefficient.....	22
Figure 11: Moment Coefficient as a Function of Angle of Attack.....	22
Figure 12: HALE-SPUAV proposed configuration.....	23
Figure 13: Airframe Mass Prediction Models.....	26
Figure 14: Correlation between aircrafts speed and power index.....	28
Figure 15: JavaProp Propeller Parameters Utilized on the HALE-SPUAV.....	31
Figure 16: Aircraft with Ailerons.....	35
Figure 17: Ailerons with Dimensions in Feet.....	35
Figure 18: XFLR5 Reynolds Number Legend (NACA0012).....	38
Figure 19: Lift/Drag Ratio as a Function of Angle of Attack (NACA0012).....	38
Figure 20: Lift Coefficient as a Function of Angle of Attack.....	38

Figure 21: Moment Coefficient as a Function of Angle of Attack.....	38
Figure 22: Lift Coefficient as a Function of Drag Coefficient for NACA 0012 Airfoil.....	39
Figure 24: Solar Converters Inc MPPT.....	41
Figure 23: SunSaver MPPT Charge Controller SS-15.....	42
Figure 25: Mars Electric LLC PMAC Motor.....	43
Figure 26: Aircraft CG Locations.....	44
Figure 27: Nastran Model to study vertical load.....	46
Figure 28: Vertical displacement of the Wing due to battery load.....	46
Figure 29: Lift Coefficient as a Function of Angle of Attack for NACA 0012 Airfoil.....	48
Figure 30: Lift Coefficient as a Function of Angle of Attack for Selig 1223 Airfoil.....	48

LIST OF TABLES

Table 1: Classification of UAVs.....	7
Table 2: Important design parameters for similar aircrafts.....	16
Table 3: Aircraft Weight Estimates.....	27
Table 4: Critical mission parameters.....	27
Table 5: Wing Geometry Values.....	33
Table 6: Dimensions for stabilizers.....	39
Table 7: Mars Electric LLC PMAC Motor Specs.....	43
Table 8: Component Center of Gravity.....	45
Table 9: Static Margin Variables and Definitions.....	47
Table 10: Drag Polar Comparison.....	51

1.0 INTRODUCTION

1.1 MOTIVATION

Today there are more than 11,000 UAVs in service (or planned service) by the United States Military for various purposes. Although these UAVs provide tremendous benefits, they fall short on performance due to their power restrictions; they must either land to be recharged or land for another UAV to complete the mission. By having the UAV returning every two (2) hours for recharge can be extremely costly or dangerous for the war fighter, if used on the battlefield [1].

Increasing battery sizes or the number of batteries, due to the weight restrictions, cannot solve these problems; weight is proportional to the endurance of the UAV. With the implementation of solar cells, the UAV would be able to collect and store solar energy to be used for night time flight, and thus having no return to recharge (R/R) requirement. Again efficiency would play a drastic role; all the critical sub-systems must be lightweight and efficient enough to support the total weight of the UAV.

Without an R/R requirement a war fighter can always depend on the UAV being able to scan a perimeter prior to entry. Currently, the U.S. military has been looking for a long endurance low cost surveillance aircraft, similar to this mission (as defined in Section 3.0) [2]. This design may not only be used for military purposes, but weather surveillance, and even commercial use.

1.2 OBJECTIVE

The objective of this mission is a proof of concept, to be implemented into a fully functional prototype upon approval for specific military and commercial use. The aircraft's performance will be highly affected by the efficiencies of the sub-systems. This UAV will be initially required to:

- Stay aloft for 4 days (96 hours) minimum
- Maintain 75,000 ft max. altitude (day time)
- Maintain 40,000 ft min. altitude (night time)
- Support a 100 lbs payload (excluded from weight of components)
- Achieve autonomous flight (after lift off)
- Return safely without any major damage to body or components

With respect to the mission requirements, the SPUAV shall be able to completely recharge the onboard batteries using the equipped solar panels. At no time during the flight is the SPUAV to R/R. The SPUAV shall be able to maintain enough stored energy after its return to be able to be re-used within 24 hours maximum (if required). If grounded for long than 24 hours, a recharge is recommended.

1.3 LITERATURE REVIEW

In this section, a brief history of solar powered aircraft will be discussed, as well as other UAV electric vehicle studies that have been done over the last 30 years. Detailed mission specification and performance data for the solar powered UAVs that will be discussed are shown in Appendix A [1].

1.3.1 UAV

Unmanned Aerial Vehicles, or UAVs, as they have sometimes been referred to, have only been in service for the last 60 years. UAVs are now an important addition to many countries air defenses [1,2]. Modern UAVs have come a long way since the unmanned drones used by the USAF in the 1940s. These drones were built for spying and reconnaissance, but were not very efficient due to major flaws in their operating systems. Over the years UAVs have been developed into the highly sophisticated machines in use today. Modern UAVs are used for many important applications including coast watch, news broadcasting, and the most common application, defense [3].

1.3.2 UAV History and Timeline

The concept of unmanned aerial vehicles was first used in the American Civil War, when the North and the South tried to launch balloons with explosive devices that would fall into the other side's ammunition depot and explode [2]. The Japanese for around a month in World War II also used this concept, when they tried to launch balloons with incendiary and other explosives. The idea was that high-altitude winds would carry them to the United States, where the dropping bombs would cause panic. Apparently, both these ideas were not effective [2].

The United States did use a prototype UAV called Operation Aphrodite in World War II. It was an attempt to use manned vehicles in an unmanned mode. However, at that time, the US did not have the technology to launch or control the aircraft.

Today's UAVs owe much to the design of the cruise missiles that were used in World War II by the US and British forces. At the close of World War II, Chance Vought Aircraft, a company with no missile experience, was contracted to develop new machines. What won Vought the contract was that the proposed test missile would have a landing gear, which would help save cost. This was the beginning of the UAV [4].

USE OF UAV:

In the 1960s, the US started to develop 'drones', which were unmanned vehicles built for spying and reconnaissance. This was after they lost a manned spy aircraft to the Russians and a U-2 to Cuba. The first such drone was the 'Firebee' drone, a jet propelled by an engine made by Ryan Aeronautical Company. They were initially used heavily over Communist China in the 1960s, when major flaws were discovered and corrected [1-3].

The Vietnam War was the first time that UAVs, the drones in particular, were used extensively in reconnaissance and combat roles. A large number of Firebee drones, were launched for simple day reconnaissance activities. At first, they had simple cameras on them. Later, they were equipped with night photos, communications and electronic intelligence.

Over the last few years, it has been Israel that has been responsible for much of the development that has happened in the UAV sector. The Hunter and the Pioneer, which are used extensively by the US military, are direct derivatives of Israeli systems. The Pioneer was used in the Gulf War to good effect.

Following the Gulf War, officials recognized the importance of unmanned

systems. The Predator, first an Advanced Technology Demonstration Project, demonstrated its worth in the skies over the Balkans [4]. Some of the current versions of the Predator are loaded with Hellfire missiles for attack purposes.

Another popular UAV is the Global Hawk. This is a jet powered UAV that was used effectively in Afghanistan. It operates at around 60,000 feet, and carries a wide range of sensors [5].

UAVs that are in use and under development are both long-range and high-endurance vehicles. The Predator, for instance, can stay in the air for around 40 hours. The Global Hawk can stay in the air for 24 hours [1,2].

TIMELINE [1,2]:

1922 – First Launch of an unmanned aircraft (RAE 1921 Target) from an aircraft carrier (HMS Argus).

1924, 3 September – First successful flight by a radio controlled unmanned aircraft without a safety pilot onboard; performed by the British RAE 1921 Target 1921, which flew 39 minutes.

1933 – First use of an unmanned aircraft as a target drone; performed by a Fairey Queen for gunnery practice by the British Fleet in the Mediterranean.

1944, 12 June – First combat use of an unmanned aircraft (German Fi-103 “V-1”) in the cruise missile role.

1944, 19 October - First combat use of an unmanned aircraft (U.S. Navy TDR- 1 attack drone) in the strike role, dropping 10 bombs on Japanese gun positions on Ballale Island.

1946, 2 April – First use of unmanned aircraft for scientific research; performed

by a converted Northrop P-61 Black Widow for flights into thunderstorms by the U.S. Weather Bureau to collect meteorological data.

1955 – First flight of an unmanned aircraft designed for reconnaissance; performed by the Northrop Radioplane SD-1 Falconer/Observer, later fielded by the U.S. and British armies.

1960, 12 August – First free flight by an unmanned helicopter; performed by the Gyrodyne QH-50A at NATC Patuxent River, Maryland.

1998, 21 August – First trans-Atlantic crossing by an unmanned aircraft; Performed by the Insitu Group's Aerosonde Laima between Bell Island, Newfoundland, and Benbecula, Outer Hebrides, Scotland.

2001, 22-23 April – First trans-Pacific crossing by an unmanned aircraft; performed by the Northrop Grumman Global Hawk "Southern Cross II" between Edwards AFB, California, and RAF Edinburgh, Australia.

1.3.3 Classification of UAVs

UAVs are being classified here in their main 4 categories: micro/mini UAVs (MAV/mini), typical UAVs (TUAVs), strategic UAVs, and special task UAVs where only decoy and lethal are currently flying [4].

Table 1: Classification of UAVs

	Category (acronym)	Maximum Take Off Weight (kg)	Maximum Flight Altitude (m)	Endurance (hours)	Data Link Range (Km)	Example	
						Missions	Systems
Micro/Mini UAVs	Micro (MAV)	0.10	250	1	< 10	Scouting, NBC sampling, surveillance inside buildings	Black Widow, MicroStar, Microbat, FanCopter, QuattroCopter, Mosquito, Hornet, Mite
	Mini	< 30	150-300	< 2	< 10	Film and broadcast industries, agriculture, pollution measurements, surveillance inside buildings, communications relay and EW	Mikado, Aladin, Tracker, DragonEye, Raven, Pointer II, Carolo C40/P50, Skorplo, R-Max and R-50, RoboCopter, YH-300SL
Tactical UAVs	Close Range (CR)	150	3,000	2-4	10-30	RSTA, mine detection, search & rescue, EW	Observer I, Phantom, Copter 4, Mikado, RoboCopter 300, Pointer, Camcopter, Aerial and Agricultural RMax
	Short Range (SR)	200	3,000	3-6	30-70	BDA, RSTA, EW, mine detection	Scorpio 6/30, Luna, SilverFox, EyeView, Firebird, R-Max Agri/Photo, Hornet, Raven, phantom, GoldenEye 100, Flight, Neptune
	Medium Range (MR)	150-500	3,000-5,000	6-10	70-200	BDA, RSTA, EW, mine detection, NBC sampling	Hunter B, Mucke, Aerostar, Sniper, Falco, Armor X2, Smart UAV, UCAR, Eagle Eye+, Alice, Extender, Shadow 200/400
	Long Range (LR)	-	5,000	6-13	200-500	RSTA, BDA, communications relay	Hunter, Vigilante 502
	Endurance (EN)	500-1,500	5,000-8,000	12-24	> 500	BDA, RSTA, EW, communications relay, NBC sampling	Aerosonde, Vulture II Exp, Shadow 600, Searcher II, Hermes 450S/450T/700
	Medium Altitude, Long Endurance (MALE)	1,000-1,500	5,000-8,000	24-48	> 500	BDA, RSTA, EW weapons delivery, communications relay, NBC sampling	Skyforce, Hermes 1500, Heron TP, MQ-1 Predator, Predator-TT, Eagle-1/2, Darkstar, E-Hunter, Dominator
Strategic UAVs	High Altitude, Long Endurance (HALE)	2,500-12,500	15,000-20,000	24-48	> 2,000	BDA, RSTA, EW, communications relay, boost phase intercept launch vehicle, airport security	Global Hawk, Raptor, Condor, Theseus, Helios, Predator B/C, Libellule, EuroHawk, Mercator, SensorCraft, Global Observer, Pathfinder Plus,
Special Task UAVs	Lethal (LET)	250	3,000-4,000	3-4	300	Anti-radar, anti-ship, anti-aircraft, anti-infrastructure	MALI, Harpy, Lark, Marula
	Decoys (DEC)	250	50-5,000	< 4	0-500	Aerial and naval deception	Flight, MALD, Nulka, ITALD, Chukar
	Stratospheric (Strato)	TBD	20,000-30,000	> 48	> 2,000	-	Pegasus
	Exo-stratospheric (EXO)	TBD	> 30,000	TBD	TBD	-	MarsFlyer, MAC-1

Micro and Mini UAVs: Micro and mini UAVs comprise the category of the smallest platforms that also fly at lower altitudes (under 300 meters). Designs for this class of device have focused on creating UAVs that can operate in urban canyons or even inside buildings, flying along hallways, carrying listening and recording devices, transmitters, or miniature TV cameras. The U.S. Defense Advanced Research Projects Agency (DARPA) has developed a set of criteria with which to distinguish of vertical take off and landing (VTOL) in the near future

micro UAVs are expected to become more practical and prevalent. Thus, the prospects are good for micro and mini UAVs to become intelligent “aerial robots,” that is, fully autonomous thinking machines [4].

Tactical UAVs: This category includes heavier platforms flying at higher altitudes (from 3,000 to 8,000 meters). Unlike micro and mini UAVs, which are mostly used for civil/commercial applications, tactical UAVs primarily support military applications.

Strategic UAVs: HALE platforms are strategic UAVs with a MTOW varying from 2,500 kilograms up to 12,000 kilograms and a maximum flight altitude of about 20,000 meters. They are highly automated, with takeoffs and landings being performed automatically. At any time during its mission the ground control station (GCS) can control the HALE UAV. Northrop Grumman’s military UAV, the Global Hawk, with 35 hours of endurance is probably the most wellknown HALE UAV and offers truly remarkable performance.

An example of a non-military HALE is the electric/solar-powered Helios, which is some how similar to SPUAV-HALE, from Aerovironment operated by NASA. The Helios uses solar panels to power electrically driven propellers and has set an altitude record of about 98,500 feet. This UAV’s design offers many attractive features for civil tasks, such as Earth observation augmenting and complementing remote sensing satellites. Other HALE UAV applications include communications, mapping, and atmospheric monitoring.

1.4 SOLAR FLIGHT

Sunrise I: The first recorded solar flight was achieved by Astro Flight's Sunrise I in 1974. It was powered from PV cells mounted on the top surface of its wings, capable of a maximum of 450 W. It weighed 27.5 lb, and had a 32 ft wingspan. Sunrise I was damaged in a sand storm in 1975 [2].

Gossamer Penguin :In 1980, AeroVironment flew the solar powered Gossamer Penguin above Rogers Dry Lakebed at Edwards, California. This aircraft was manned, weighed 68 lb without the pilot, used 600 W of power from solar cells, had a wingspan of 71 ft, and made numerous flights. Its solar panels were fixed at an angle to achieve high solar energy capture, as shown in Figure 1 [2].

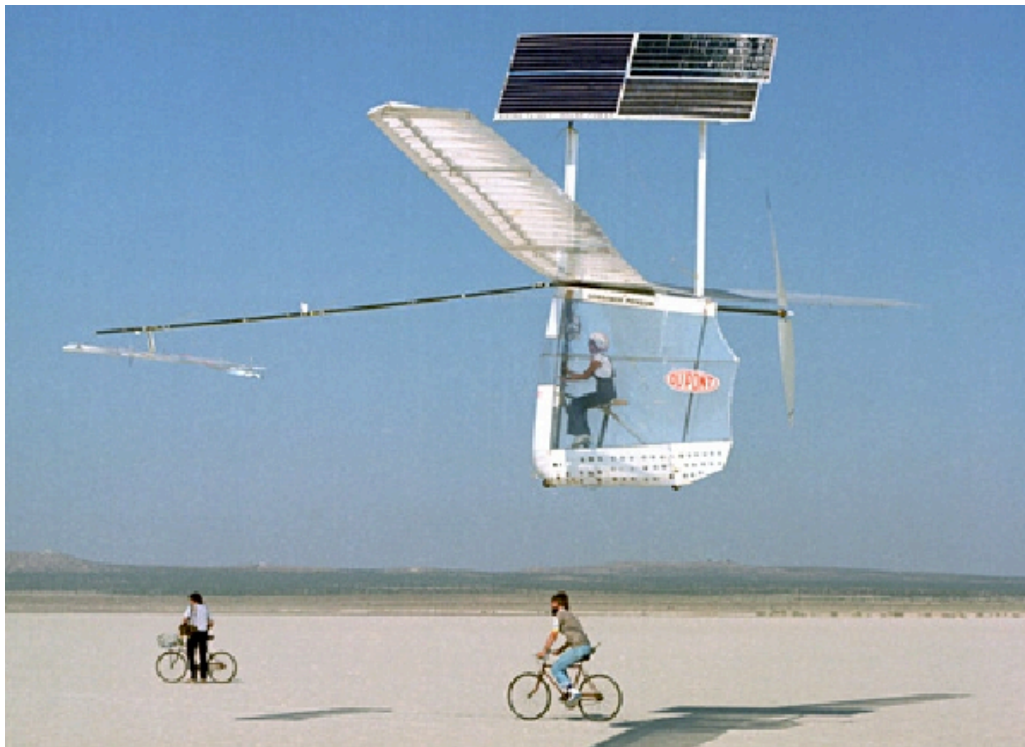


Figure 1: NASA-funded Gossamer Penguin by AeroVironment

Pathfinder: AeroVironment was funded in 1981 to work on a classified solar powered UAV project for the U.S. government. They built HALSOL (High-Altitude

Solar Energy), a UAV that was mothballed for about a decade. HALSOL later evolved into the solar UAV entitled Pathfinder, shown in Figure 2. Pathfinder could produce a maximum of 8,000 W from solar cells, weighed 486 lbs, and had a wingspan of 98 ft. In the mid 1990's, NASA's Environmental Research Aircraft and Sensor Technology (ERAST) program became interested in solar aircraft and Pathfinder became a part of NASA's ERAST program. On Sept. 11, 1995, Pathfinder set an altitude record for solar aircraft by climbing to 50,500 ft. The National Aeronautic Association presented the NASA- industry team with an award for one of the "10 Most Memorable Record Flights" in 1995. Pathfinder set the world altitude record for both propeller driven aircraft and solar powered aircraft in 1997 with an altitude of 71,530 ft. Pathfinder was later modified by an increase of wingspan to 121 feet and a replacement of the old PV cells with newer, more efficient cells. This increased the maximum power potential by another 4,500 W. This version, called Pathfinder Plus, flew to an altitude of 80,000 ft. in 1998 [3].



Figure 2: NASA Pathfinder Plus

Centurion: AeroVironment created Centurion in 1998 (Figure 3). Centurion had a wingspan of 206 ft, weighed 1,300 lbs, and was powered with a PV array capable of capturing a maximum of 31 kW of solar power [4].



Figure 3: NASA Centurion

Helios: The latest of the larger NASA funded AeroVironment solar planes was Helios (Figure 4). Helios set an impressive altitude record of 96,500 ft in the summer of 2001. It had a wingspan of 247 ft, weighed over 2,000 lbs, and was powered by a PV array capable of capturing 42 kW of solar power [4]. One hour into a planned 20-hour test flight, Helios crashed into the Pacific Ocean and was destroyed in June 2003 [5].



Figure 4: NASA Helios

PicoSol: The smallest solar powered aircraft that is known to have successfully flown is the PicoSol radio controlled airplane by Dr. Sieghard Dienlen. This small aircraft weighed 1.24 N and had a wingspan of .99 m [4].

SoLong: AC Propulsion's Solar Electric Powered SoLong UAV [5] flew for 48 continuous hours. SoLong was the first solar powered UAV of its size and class to successfully fly through the night and fully recharge its batteries during the day from the sun's power while remaining airborne. This feat was only accomplished in a desert with consistent thermals in the day, a time of year and location where high solar flux across the surface of the solar cells can be achieved, and by a team of skilled pilots taking turns in the "cockpit" from their ground station.

SoLong had a nominal solar power capability of 225 W, a wingspan of 4 meters, a weight of 12.6 kg, and used a Maximum Power Point Tracker (MPPT) developed by AC propulsion that weighed 100 grams.

2.0 MISSION SPECIFICATION

2.1 MISSION PROFILE

The mission profile for this mission is shown in Figure 5. The details for each phase of the profile are discussed below:

- Phase 1: UAV motor will turn on and start taxi.
- Phase 2: Take off at 4AM.
- Phase 3: After six hours of climbing, the UAV will cruise at 50,000 ft to recharge batteries enough to make the final climb.
- Phase 4: After three hours of direct sunlight (between 10AM and 1PM), the UAV will begin to climb to cruise altitude of 75,000 ft.
- Phase 5: UAV at cruise altitude at 4PM. At cruise, the UAV will use the rest of the day to charge batteries.
- Phase 6: UAV begins descent at 9PM. UAV will rely on onboard batteries to stay in air.
- Phase 7: At 5AM, the UAV cruises at an altitude of 40,000 ft for three hours to charge the batteries partially.
- Phase 8: At 8AM, UAV begins climb to 50,000 ft.
- Phase 9: At 12PM, UAV cruises for two hours. This will recharge batteries during direct sunlight.
- Phase 10: At 2PM, UAV begins climb to 75,000 ft.
- Phase 11: At 4PM, UAV cruises at 75,000 ft until sundown to charge batteries.
- Phase 12 through 17: Repeat phases 6 through 11.

- Phases 18 through 23: Repeat phase 6 through 11.
- Phase 24: At 9PM, after four consecutive days in flight, UAV beings descent back to ground only using minimum power.
- Phase 25: At 8AM, UAV lands on runway.
- Phase 26: UAV finishes taxi and powers down.

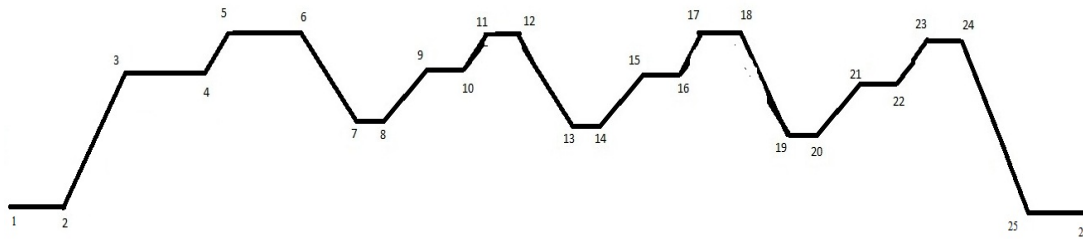


Figure 5: Mission Profile for HALE-SPUAV

2.2 MARKET ANALYSIS

The primary motivation behind building such an aircraft is the push for greener aviation. Over the last several years many aerospace companies, including Boeing, NASA, and LM, have invested in alternative fuel technology and UAVs. The solar impulse (longer range) and Zephyr's (longer endurance) achievements have increased the popularity for solar-powered UAVs, thus creating a large market for such technology. There has also been a need for studying and providing alert for various natural disasters such as wildfire. UAV such as HALE-SPUAV discussed in the report, would be an asset to them. It can also be used in many military and surveillance application around the globe. The advancement in technology may also achieve its space applications such as Marsh surface monitoring.

2.3 TECHNICAL AND ECONOMICAL FEASIBILITY

Although solar power UAVs are more expensive to build and research because of the advanced technology used, they would be more fuel-efficient and would require less maintenance than the fueled UAVs. Since the solar-powered UAV will not require any jet fuel, it can save millions of dollars over a long period of time and help save the environment.

Since the development of NASA's Helios, only problem that has remained prominent is the weight of the batteries required for powering the UAV. Development of Lithium-Sulfur batteries allowed us to reduce the total weight by 50-60 percent with the highest value of energy density. Building the aircraft will be relatively simple since all other products are available in the market such as solar cells, motors, and avionics.

2.4 CRITICAL MISSION REQUIREMENTS

The critical mission requirements that will drive the design of the aircraft are as follows

- Total endurance will be no less than 96 hours
- Must be capable to achieve cruise altitude of 75000 ft

3.0 COMPARATIVE STUDY OF SIMILAR AIRPLANES

In this section the airplanes that will be studied are Sunrise, Solar challenger, Pathfinder plus, Centurion, Helios, Solae impulse, Zephyr, and sky sailor.

3.1 MISSION CAPABILITIES AND CONFIGURATION SELECTION

The mission capabilities and configuration selection for the studied aircrafts are shown in appendix A. As you can see, most of the capabilities of these

aircrafts are minimal and used primarily to study the potential of solar powered long endurance and high altitude flight. Most of the aircraft have closed to flying wing configuration with multiple propeller driven engines.

3.2 COMPARISON OF IMPORTANT DESIGN PARAMETERS

The important design parameters are shown in table 2. The complete list of design parameters for the aircrafts that were studied can be found in appendix A. If the solar impulse excluded, the total weight of each aircraft does not exceed 2400lb without implementation Li-Su batteries. So weight of HALE-SPUAV should be remarkably low after using these batteries. No aircraft exceed wingspan of 240ft and most of them can go up to 75000ft during cruise. Therefore, to build a successful SPUAV a low weight design with high aspect ratio and relatively high wingspan is necessary.

Table 2: Important design parameters for similar aircrafts

UAV	Sunrise (1974)	Solar challenger (1981)	Pathfinder plus (1988)
Weight (lb)	27	200	700
Wingspan (ft)	32	47	121
Max power (KW)	12	8.8	12.5
Ceiling (ft)	8000(projected 28000)	14,300	80,201
Endurance			14-15 hrs

UAV	Helios HPO3 (2001)	Solar impulse (2009)	Zephyr (2010)	Sky sailor (2006)
Weight (lb)	2320	3500	117	12
Wingspan (ft)	247	208	74	11
Max power (KW)	31	30		
Ceiling (ft)	96,863	39,000	70,000	1640
Endurance	24hrs	36hrs (projected)	336 hrs 22 min	

4.0 COMPARATIVE STUDY OF THE AIRPLANE WITH THE SIMILAR MISSION PERFORMANCE

The configuration and capabilities of similar airplane are shown in shown in table 2. These aircraft consist of a multiple engine propeller propulsion system. This was chosen because current technology allows propeller to be powered by electric motors, which requires no gas and are required for solar powered aircrafts. The high wing configuration is chosen because of weight saving and to keep the wings far away from the ground to reduce the damage. Since the wing has PV cells and batteries, it becomes the most expensive part of the aircraft; thus, avoiding damage to the wing is priority. Also, it provides solar cells with maximum exposure to sunlight.

For the empennage, there are three options that are most common to solar power aircraft: V-tail, t-tail, and conventional. The t-tail will provide more area to

put the solar cells then any other and its less heavy then conventional tail configuration.

5.0 SELECTION OF PROPULSION SYSTEM

The propulsion system type will be electrical with photovoltaic cells powering the motors and payload.

5.1 SELECTION OF NUMBER OF ENGINES

Looking at the power requirements there will be multiple engines on the tip of the wing. The distance between each engine will depend on wing loading and dihedral of the wing.

5.2 PROPELLER SIZING

The propeller sizing can vary depending upon the diameter of the fuselage. The larger the propeller diameter the more efficient the propeller becomes. One of the limitations that Raymer [7] discusses is the propeller tip speed, which is the sum of the rotational speed and the aircraft's forward speed, as shown in (5.1) and (5.2).

$$(V_{tip})_{static} = \pi nd / 60 \quad (5.1)$$

$$(V_{tip})_{helical} = \sqrt{(V_{tip}^2 + V^2)} \quad (5.2)$$

To determine the propeller diameter, Roskam [8] uses data from other aircraft and (5.3) to determine the ideal propeller diameter based on maximum power per engine, number of propeller blades, and the power loading per blade.

$$D_p = \left[\frac{4 p_{max}}{\pi n_p p_{bl}} \right]^{1/2} \quad (5.3)$$

A propeller, which is readily available at the time of the manufacturing, would be ideal. For the initial selection, propeller with 70 in diameter with advance composite material will be selected. Design would take high altitude laminar flow into consideration as its ambient condition.

6.0 CONFIGURATION SELECTION

6.1 OVERALL CONFIGURATION

Based on Roskam, conventional configuration is used for the HALE-SUPAV. The UAV will not have higher range and thus will preliminary fly on land and if necessary on water. Adding another alternative fuel system would give more rang but will also increase complexity and weight, which is not recommended.

6.2 WING CONFIGURATION

The wing selection is a vital part for a HALE-SPUAV because not only should the wing have good aerodynamic characteristics, but it also must be suitable for solar cells to be added on to the top of the surface of the wing. For this UAV, a high cantilever wing will be selected primarily for simplicity and to provide enough clearance during landing. A high wing also provides lateral stability, which is needed since there will be minimal stabilizing devices on this type of aircraft. The geometry of the wing should have negligible sweep because the aircraft will be operating at low speeds. Sweep will also increase weight and reduce available solar cell area, both of which will hinder the aircraft's performance. An initial airfoil selection will be the Selig 1223, as shown in Figure 6. This airfoil has 12.14% maximum thickness-to-chord ratio at roughly 20% from the leading edge.

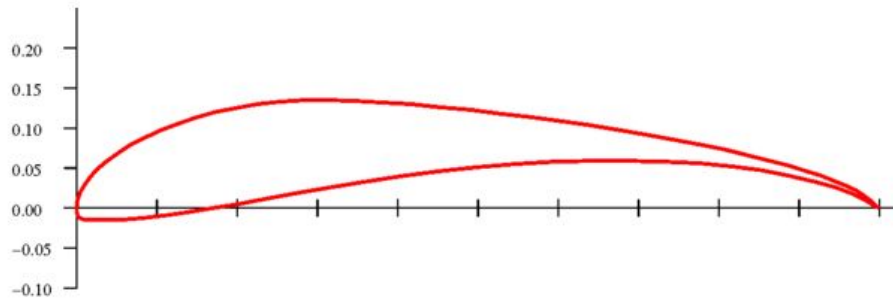


Figure 6: Selig 1223 Airfoil with Unit Length

The Selig 1223 airfoil was chosen as the initial configuration because it has all the characteristics, which requires in solar power high altitude and long endurance airplanes. The first important one is that it is a low Reynolds number airfoil. Since this UAV will be flying at low speeds, a low Reynolds number will be generated throughout the mission, and therefore an airfoil that has ideal characteristics at low speed has been chosen. High lift to drag ratio is also one of the important characteristics. Using XFLR5 software that analyses the airfoils, a graph of L/D vs. angle of attack was created and is shown in Figure 8. A legend that is used for the different Reynolds number used is shown in figure 7. As the figures show, not only does this airfoil have a high lift-to-drag ratio, but also it has a fairly wide operating angle of attack where the lift-to-drag ratio is optimum. Other airfoil characteristics are shown in Figures 9, 10, 11.

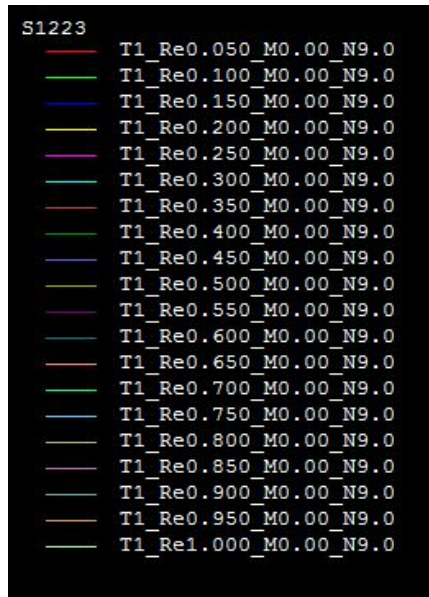


Figure 7: XFLR5 Reynolds Number Legend (0.050 is 50000, 0.1 is 100,000, etc.)

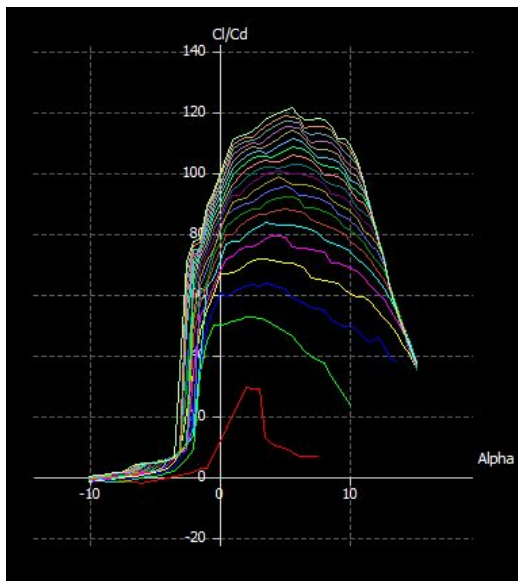


Figure 8: Lift-to-Drag Ratio
as a Function of Angle of Attack

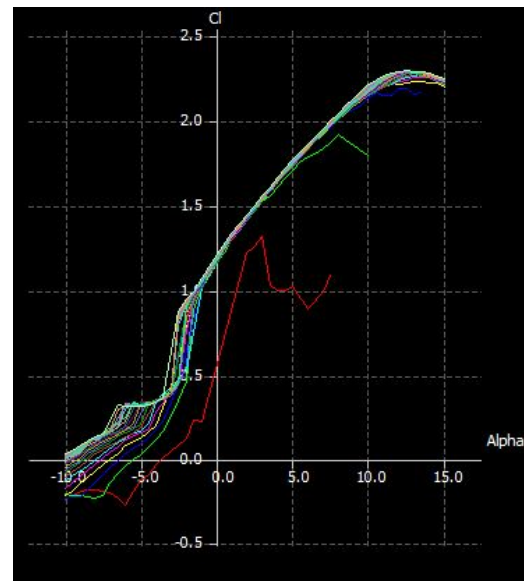


Figure 9: Lift Coefficient
as a Function of Angle of Attack

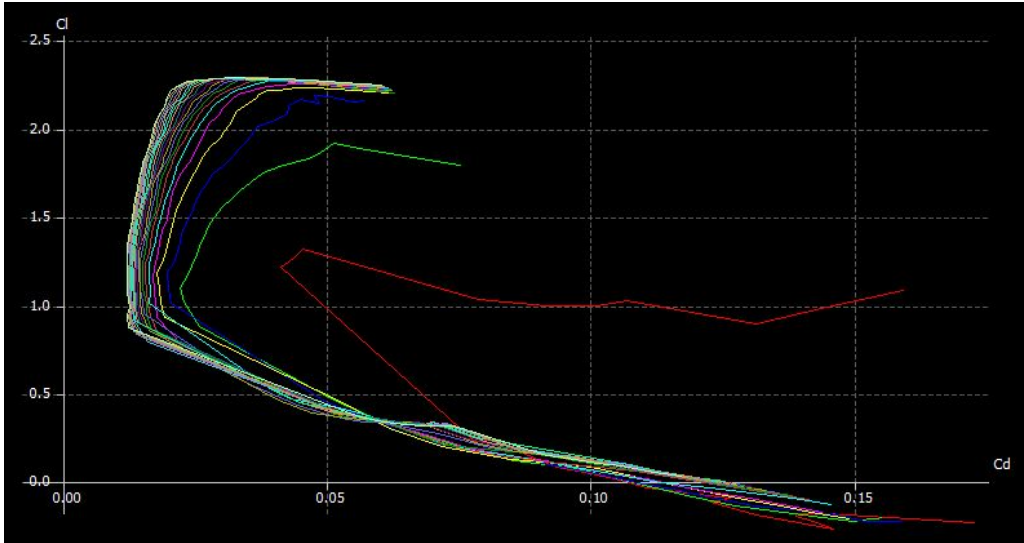


Figure 10: Lift Coefficient as a Function of Drag Coefficient

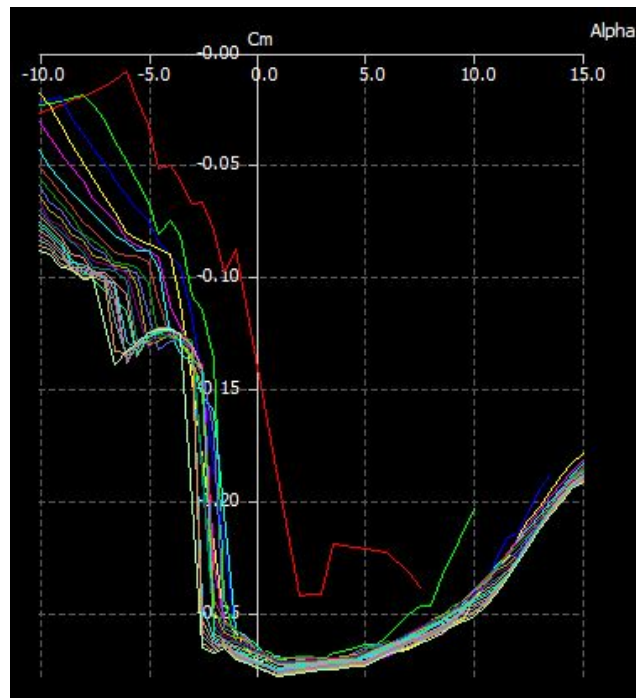


Figure 11: Moment Coefficient as a Function of Angle of Attack

The aircraft will have no geometric or aerodynamic twist because it needs to absorb as much solar energy as possible, and optimum geometry to do that would require no wing twist. Due to longer wingspan and battery weight, aircraft will have dihedral and winglets in the final configuration. Aircraft will not have any high lift devices, as it will add up more weight.

6.4 EMPENNAGE CONFIGURATION

The HALE-SPUAV will incorporate a t-tail empennage configuration because it is easy to build and provides more area for solar cells. V-tail might be lighter in weight but getting maximum solar power is essential for the mission. Thus t-tail would be the ideal choice.

6.3 LANDING GEAR DISPOSITION

This aircraft will have two landings gear installed. Main landing gear would be on fuselage and smaller one will be in tail section for support. The skid will also be considered upon the length of the wing for supporting the wing tips.

6.4 PROPOSED CONFIGURATION

Figure 12 shows one of the proposed configurations. For simplicity, a cylindrical fuselage is chosen for an initial configuration. The t-tail empennage, as well as the high wing configuration, will be the same for all configurations. The taper wing is been considered to increase the aspect ratio effect and associated structural changes should be done if needed during the design.

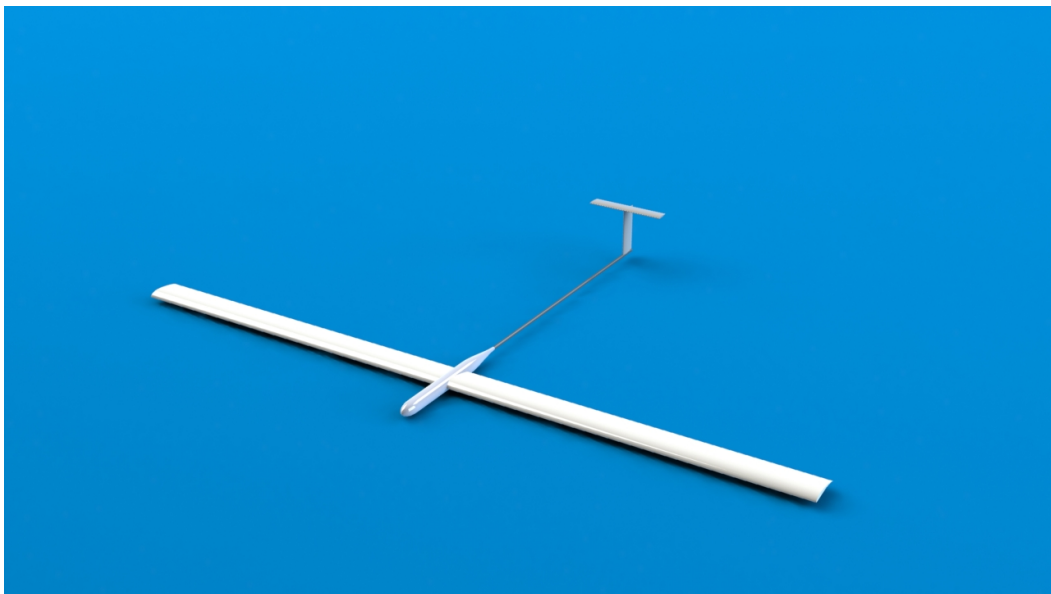


Figure 12: HALE-SPUAV proposed configuration

7.0 MISSION WEIGHT ESTIMATES

7.1 COMMENTS

Before the calculation of the weights is determined, a few factors should be considered: The weight of solar powered aircrafts differ from the weight of the fuel power aircrafts thus the method to determine it. In most common aircraft, fuel weight is an important variable when calculating the takeoff weight versus the empty weight. Since this UAV runs on PV cells, there is no empty weight or fuel weight present. There for weight analysis cannot be done by using Raymer or Roskam's conventional methods. However, Noth [9] goes into detail about weight prediction models and how it is possible to obtain an appropriate estimate of the component weight simply by inserting the relative parameters that pertain to the aircraft. That's why North's method will be used for SPUAV.

7.2 SOLAR SYSTEM WEIGHTS

To begin with, power require for steady level flight is been determined. Data from other HALE SPUAVs are used and found out that at least 20 kW of power needed for this aircraft. Knowing that this aircraft will need to run on just battery power throughout the night, then approximated that I would need 240 kW-hr to have the aircraft fly continuously using just battery power. This value is an overestimation because throughout the night, we could potentially turn off the power to the engines and have the aircraft use only the wing's aerodynamic properties to float. I understand that this will result in a loss of altitude, but this is fairly consistent with other HALE SPUAVs.

Knowing that 240 kW-hr is needed, Li-Su batteries are chosen with the assumption that it will be available for commercial use by the end of the design. For an initial analysis shown in section 2.2 we chose the lithium-sulfur rechargeable batteries which would give us 400 W-hr/kg instead of normal Li-Po batteries' 200 W-hr/kg. Using the nominal capacity and voltage values, number of battery cell required can be calculated which are 968. Multiplying that value by how much each battery weighs and I ended up with 260 lbs, which seems much efficient in comparison to other HALE SPUAVs.

Once batteries have been chosen, number of solar cell and area to accomplish those solar cells will be calculated. The solar cells will be used are the Sunpower A-300 primarily because of the high efficiency. It is been calculated that approximately 610 ft² of area needed to produce 10 kW. This number comes from Honsberg & Bowden [10] model for total irradiance of 1.05 kW/m² for a 37 degree North latitude around June 18-22. The 37°north latitude corresponds with San Jose, CA. Also, according to Greentech ZONE [11], "the A-300 silicon solar cell delivers 3-kW in less than 17 square meters." Using this information, calculate that using a combination of these solar cells; we can achieve about 16.4 W/ft². To get at least 10 kW, required total area would be as follows:

$$b = \sqrt{(s * AR)} = \sqrt{(610 \text{ ft}^2) * (40)} = 156 \text{ ft}$$

Using the total solar cell area, mass of the solar cell can be calculated. We assumed that each solar cell weighs 64 mg/cm² since literature online says that the Sunpower A-300 solar cell weighs about twice as much as the RWE-32 solar

cell, which weighs 32 mg/cm². Using this data, total solar cell mass comes to 175 lbs.

7.3 AIRFRAME WEIGHT

For the airframe weight, Noth provides a statistical model, which calculates the weight of the airframe knowing the aspect ratio and wingspan. Figure 13 shows the prediction models from the analysis that Noth did.

Model	$W_{af} = f(S, AR)$	$W_{af} = f(b, AR)$	$W_{af}/S = f(W_{af}, AR)$
Noth	$0.44 S^{1.55} AR^{1.30}$	$0.44 b^{3.10} AR^{-0.25}$	$0.59 W_{af}^{0.35} AR^{0.84}$
Stender	$8.763 S^{0.778} AR^{0.467}$	$8.763 b^{1.556} AR^{-0.311}$	$16.27 W_{af}^{-0.285} AR^{0.600}$
Rizzo	$15.19 S^{0.656} AR^{0.651}$	$15.19 b^{1.312} AR^{-0.005}$	$63.24 W_{af}^{-0.524} AR^{0.992}$

Figure 13: Airframe Mass Prediction Models

The Stender model is chosen because it is most applicable to our aircraft. The Noth model is primarily for solar-powered UAVs that have a wingspan of less than 10 m, and the Rizzo model is only applicable to UAVs and not SPUAVs. If we let k_{af} , x_2 , and x_1 be similar to the Stender model, and making sure to use the correct units since the Noth model is metric, we then calculate that the airframe total weight as follows:

$$W_{af} = 8.763 S^{0.778} AR^{0.467} = 8.763 (122 m^2)^{0.778} (40)^{0.467} = 1490 N = 330 lbf$$

A value of 350 lb will be assumed for the airframe weight primarily for simplicity and to account for any tolerances from the wing area. The other component masses are fixed. For this mission, other masses would be as shown in table 3.

Table 3: Aircraft Weight Estimates

Components	Weight (in lb)
Batteries	260
Solar Cells	175
Airframe	350
Payload	100
Propulsion Group	250
TOTAL	1135

8.0 PERFORMANCE CONSTRAINT ANALYSIS

8.1 COMMENTS

From the weight estimation, we have defined a wingspan, wing area, and aspect ratio. Since these are only estimates, these values cannot be used until a performance constraint analysis is performed. The parameters shown in table 4 will be those parameters that this aircraft needs to meet during the mission.

Table 4: Critical mission parameters

Cruise Altitude	75000ft
Rate of Climb	2.08 ft/s
Maximum Cruise Velocity	27 mph
Aspect Ratio	40
Weight	1135 lb

8.2 SIZING TO CRUISE SPEED

Roskam uses a power index formula to calculate the cruise speed requirements as shown in (8.1):

$$I_p = \left[\frac{(W/S)}{\rho(W/P)} \right]^{1/3} \quad (8.1)$$

There is a graph provided in the Roskam showing the relation between power index and aircraft speed, which is shown in figure 14 here. In figure 14, a maximum cruise speed of 30 mph will result in a power index of 0.1714. This value is inserted into (8.1) to determine the relation between the wing loading (s/w) and power loading (w/p). For (8.1), the density ratio is defined at 75000ft and is 0.045.

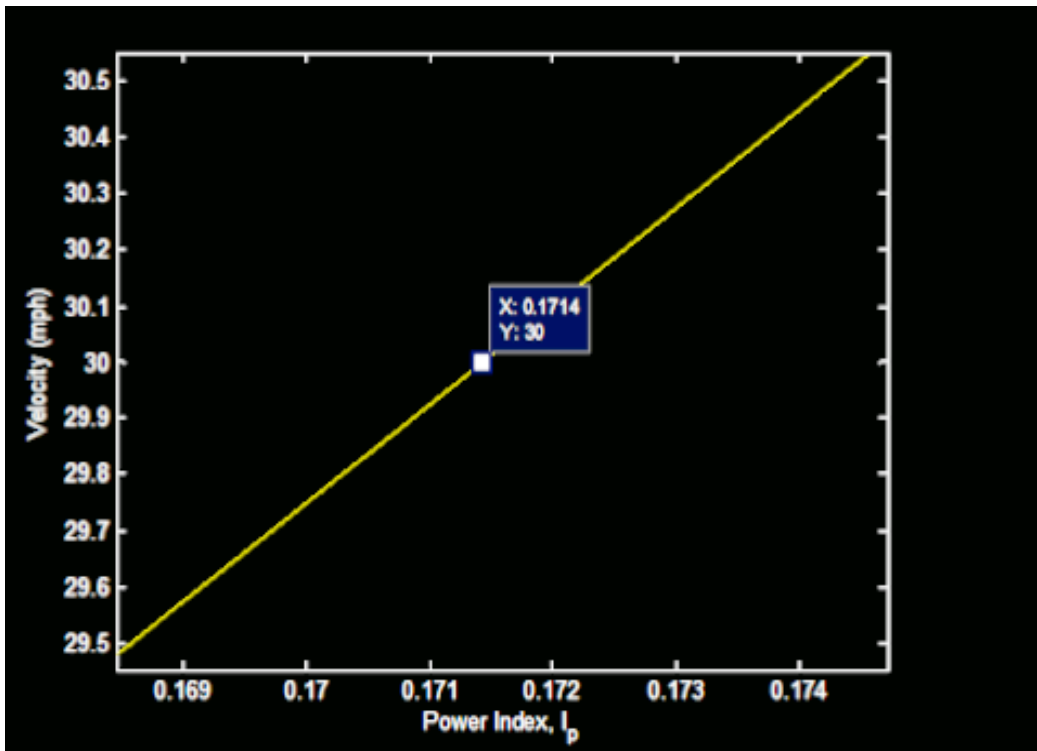


Figure 14: Correlation between aircrafts speed and power index

8.3 SIZING TO FAR23 RATE OF CLIMB REQUIREMENTS

The rate of climb requirement stated here is quite ambitious for a solar power aircraft; however, it is much lower than a conventional aircraft's climb requirement. Roskam defines the rate of climb in (8.2):

$$RCP = \frac{\eta_{plr}}{\frac{W}{P}} - \frac{\left(\frac{W}{S}\right)^{1/2}}{19 \left(\frac{C_L^{3/2}}{C_D}\right) \sigma^{1/2}} \quad (8.2)$$

A propeller efficiency of 50%, an air density ratio at 75000ft of 0.045, a lift coefficient of 1.2169, and a drag coefficient of 0.0301 are assumed. The drag coefficient was solved from the (8.3) as shown bellow [9]:

$$C_D = C_{D_0} + C_{D_{\delta}} + C_{D_{\alpha}} = C_{D_0} + C_{D_{\delta}} + \frac{C_L^2}{\pi e AR} \quad (8.3)$$

Assuming an Oswald efficiency factor of 0.9, and using the initial parameters shown in Noth's model, the total drag coefficient was calculated. A relation between our wing loading and power loading to meet our climb requirements can now be determined.

8.4 PERFORMANCE SIZING CALCULATION

Using the two correlations defined in section 8.2 and 8.3, the wing loading and power loading can be calculated analytically since they form two variable-two question system. The solution leads us to these values.

$$W/P = 1.1522, W/S = 1.79$$

Using these values power required and the wing area can be determined:

$$W/P = 1.152 \rightarrow P = \frac{W}{1.152} = 32014W$$

$$W/S = 1.79 \rightarrow S = \frac{W}{1.79} = 634 \text{ ft}$$

Using the given aspect ratio of 40, the new wingspan can be solved and which will be 156ft. Final wingspan may get little longer depending upon the taper ratio.

8.5 POWER REQUIREMENT ANALYSIS

The power available from section 8.4 was determined to be approximately 32000W. This does not take into account the efficiency of the propeller or motor that will be used. As an initial estimate, the propeller efficiency and motor efficiency will be 50% and 85% respectively. Thus, the total amount of power required can be solved for:

$$P = \left[\frac{32000W}{(0.5)(0.85)} \right] = 75294W = 75kW$$

Another approach to determine the power required for the HALE-SPUAV to maintain altitude was used also:

At steady and level flight, the thrust required is equal to the total drag and the aircraft's weight divided by the lift-to-drag ratio. The absolute maximum thrust value provided by the HALE-SPUAV's propulsion system is required during takeoff and climb and is expressed by:

$$T = D + W \sin \gamma$$

Where, γ is the climb angle of the aircraft in degrees. Assuming a rotation and climb angle of 10 degrees where the S1223 is at an optimal C_i , the maximum

total thrust required is $D + 197$ pounds. As lift to drag ratio is assumed as 40, initial thrust should be:

$$T = C_D * W + W \sin Y$$

$$T = (0.0301)(1135) + (1135)(\sin 10) = 34.1 + 197 = 231.1 N$$

To generate this much amount of thrust we need minimum 16 propeller/motor (or engine) because one engine produces 13.26lb of thrust as shown in the figure below. Thus required power is $16 * 4 = 64 kW$.

Enter Design Parameters and press the 'Design It!' button.

Propeller Name:

Number of Blades B: [-]

Revolutions per minute rpm: [1/min]

Diameter D: [m]

Spinner Dia. Dsp: [m]

Velocity v: [m/s]

Power P: [W]

shrouded rotor square tip

Propeller			
$v/(nD)$	1.833	$v/(\Omega R)$	0.584
Efficiency η	78.709 %	loading	low
Thrust T	57.24 N	Ct	0.0161
Power P	4 kW	Cp	0.0374
β at 75%R	41.2°	Pitch H	3.72 m

Figure 15: JavaProp Propeller Parameters Utilized on the HALE-SPUAV

9.0 FUSELAGE DESIGN

The fuselage geometry is relatively simple since we will not have a cockpit and the only sizing to consider will be for the payload. The payload will go at the front of the fuselage, which is 3 ft in diameter and 20 ft long, enough for any kind of payload that weighs no more than 100 lbs. Past the 20 ft area, the fuselage diameter is significantly reduced, just enough area for wiring and to hold the empennage in place. The front landing gear will be placed right where the leading edge of the aircraft is on the bottom of the fuselage. The rear landing gear is placed at the end of the fuselage, roughly 91 ft relative to the fuselage tip.

Inside the smaller diameter section of the fuselage, there will be wiring coming from the empennage. Also, the wiring that is needed for the wings will be connected to the back end of the larger diameter section of the fuselage (near the center of the aircraft). Within the space between the larger diameter and the smaller diameter, there will be the autopilot system, which is needed for this kind of application, and any extra flight control computers if necessary. See the Appendix B for CAD drawings of the fuselage.

10.0 LANDING GEAR DESIGN

The aircraft will employ a bicycle-type landing gear for minimal complexity, drag, and weight contribution as shown in Figure 15. This configuration is similar to that of the U-2 high altitude reconnaissance aircraft, B-52 bomber, and most sailplanes. Two lightweight wheels will be placed in line with each other along the longitudinal axis of the fuselage; one slightly forward of the center of lift and

the other near the aircraft's tail. To bypass complications with pneumatic tires exploding from the greatly decreased pressure at cruise altitudes, the tires will be filled with lightweight foam instead of compressed air. Appendix B shows UAV with landing gears.

11.0 WING, HIGH LIFT SYSTEM, AND LATERAL CONTROLS DESIGN

11.1 WING PLANFORM DESIGN

From the power analysis, the gross wing area was determined to be 610 square feet and the aspect ratio is 40. Throughout this section, the taper ratio, dihedral angle, sweep angle, and twist angle for our wing will be defined and calculated. Also, any high-lift devices or control surfaces that will be used on the wing will be discussed.

11.2 TAPER RATIO

Taper ratio is defined as the ratio of the wing tip chord to the wing root chord. According to Raymer, for the rectangular wings, the ideal taper ratio is 0.45 so that it “produces a lift distribution very close to the elliptical ideal” (p. 56). Therefore, taking the taper ratio into account to get lift distribution closer to elliptical. Keeping the wing area constant for solar panels and adjusted our root chord length and tip chord length. Table 5 shows the results for our straight fixed rectangular wing with no dihedral or twist.

Table 5: Wing Geometry Values

Root Chord Length	8.12 ft
Tip Chord Length	3.654 ft

Wingspan	224.06 ft
Wing Area	610 ft ²
Aspect Ratio	38.06

11.3 DIHEDRAL ANGLE

This angle on the wing is to preliminary used for increasing the dihedral effect of the aircraft. The dihedral effect is rolling moment that results from the aircraft having a non-zero sideslip angle. Thus, the dihedral is primarily used to stabilize the aircraft. For this aircraft, small amount of dihedral may be require at the end of the stability analysis.

11.4 INCIDENCE ANGLE

The incidence angle of the aircraft is the angle between the chord line of the wing and the longitudinal axis of the fuselage. This value is fixed because it depends on how the wing is mounted onto the fuselage. Looking at similar aircraft, zero or very little angle of incidence is used. Therefore for this aircraft, there will be no incident angle.

11.5 CONTROL SURFACES

The control surfaces that will be installed on the wing will be ailerons, which are devices on the trailing edge that help maneuver and control the aircraft. Since it is required to have a large lift coefficient, Raymer recommended 30% of the wingspan for the aileron length. The wing will also have trim tabs located on the ailerons so that servos would be able to move the ailerons easier. The aircraft will be using servos to control the aircraft's control surfaces that will

be able to handle this large aileron length, and will be connected to the aircraft's flight control computer in the fuselage. Using Raymer, for a 0.3 ratio of aileron span to wingspan, historical trends are for the aileron chord to be roughly 0.28-0.34 the size of the wing chord. The choice was about 20% of the wing chord because the aircraft need to have enough room for solar panels to go on the wing. Hence, decreasing the aileron chord would give it a larger area to easily install solar panels on. The aircraft with the ailerons, as well as the dimensions in feet of the aileron length, are shown in Figure 16 and 17.

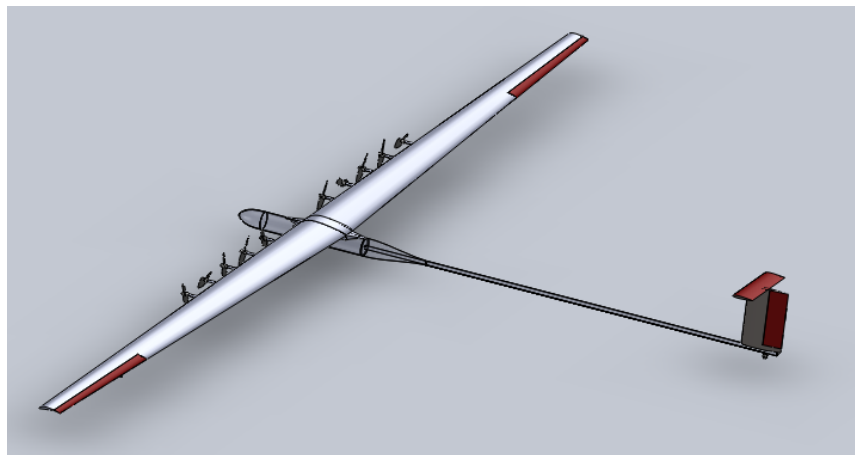


Figure 16: Aircraft with Ailerons

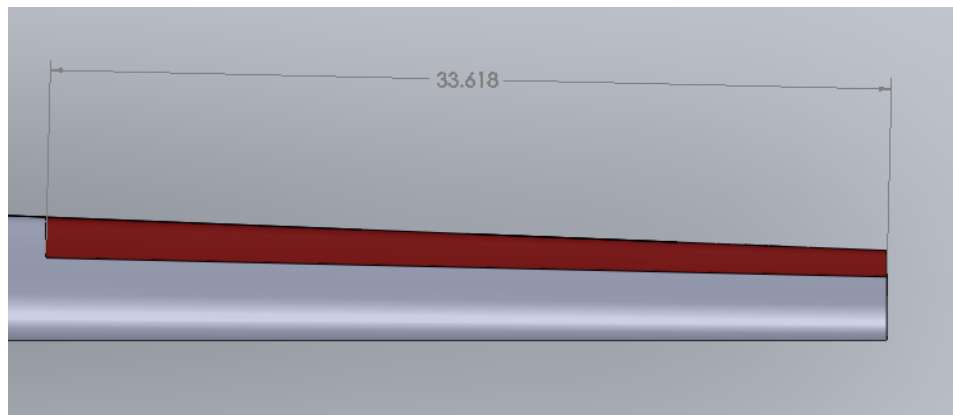
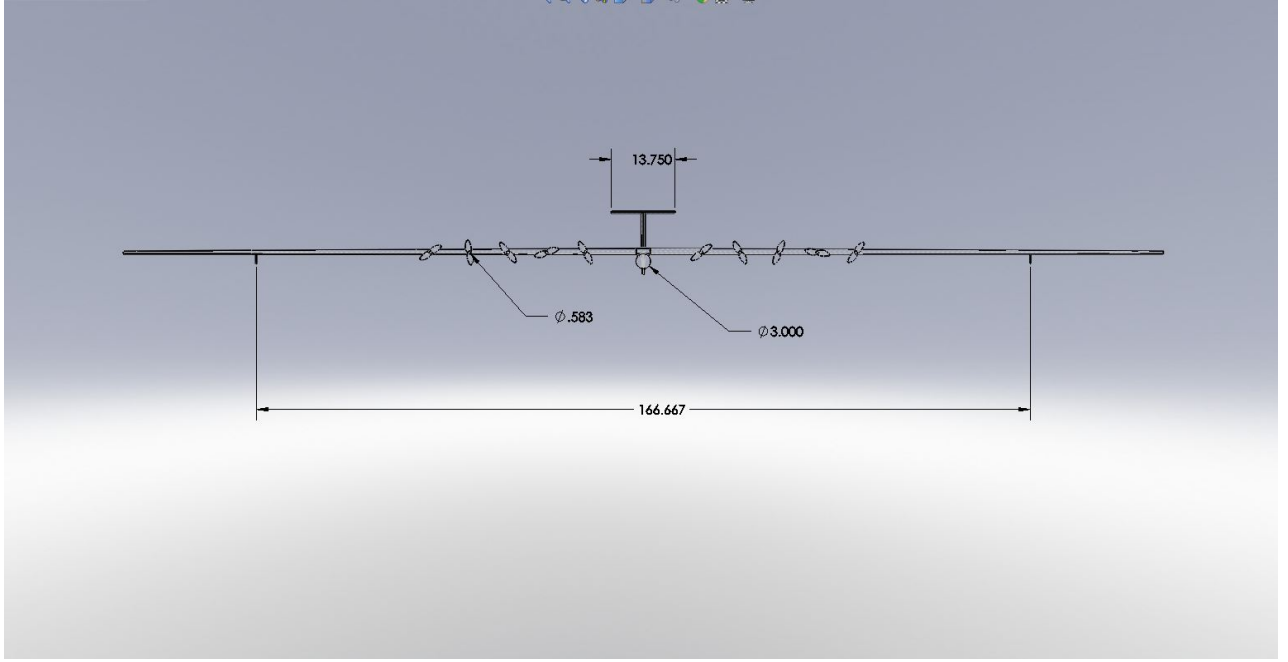


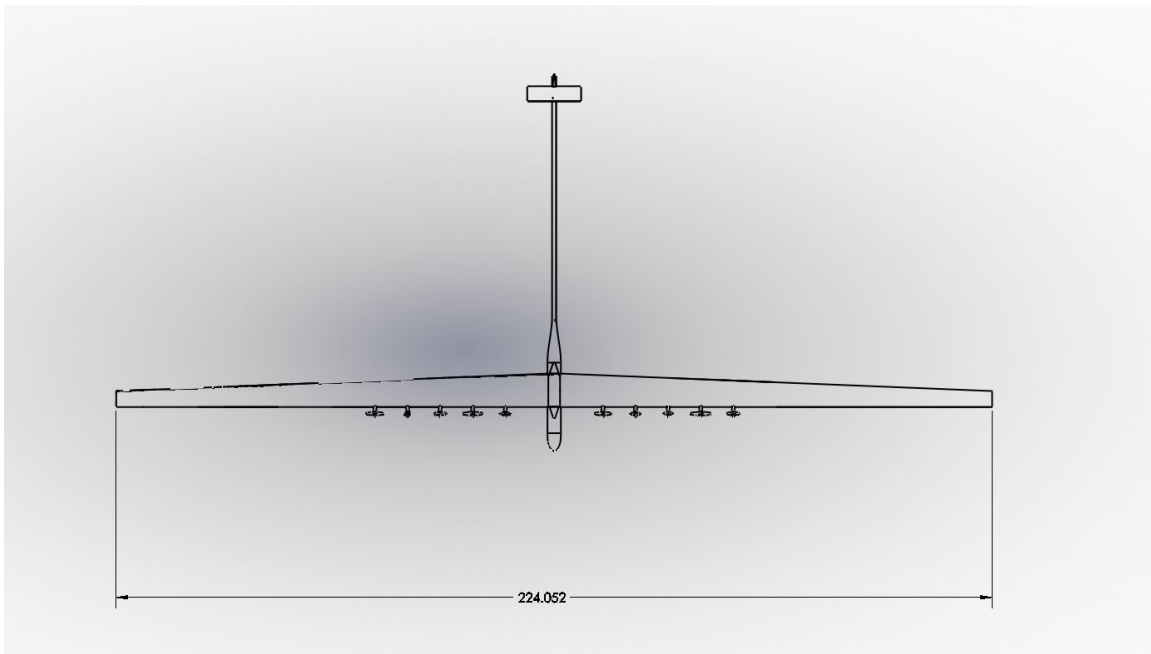
Figure 17: Ailerons with Dimensions in Feet

11.6 WING CAD DRAWING

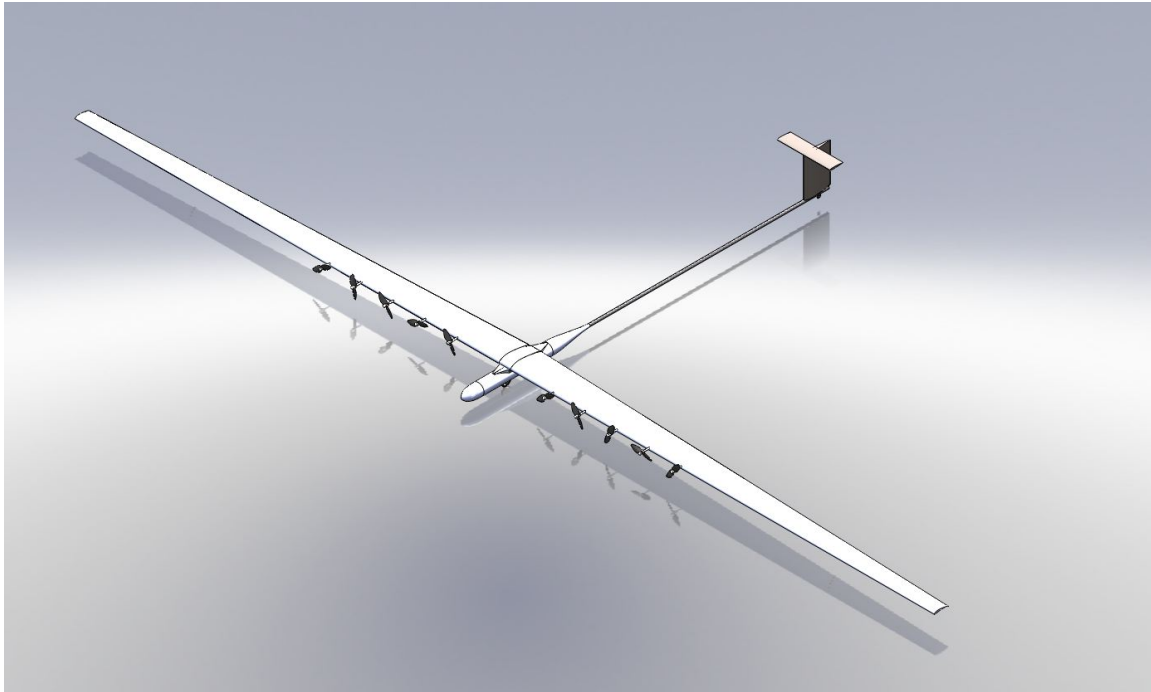
Front View



Top View



Isometric View



12.0 EMPENNAGE AND CONTROL ANALYSIS

12.1 OVERALL EMPENNAGE DESIGN

In section 6.3 it was determined that this aircraft will incorporate a t-tail empennage. This section will specify the dimensions of the empennage in more detail.

12.2 EMPENNAGE AIRFOIL

The airfoil that has been chosen is the NACA 0012 primarily for simplicity. Using XFLR5 aerodynamic properties of this airfoil can be calculated, which are shown in figure 18 through 22.

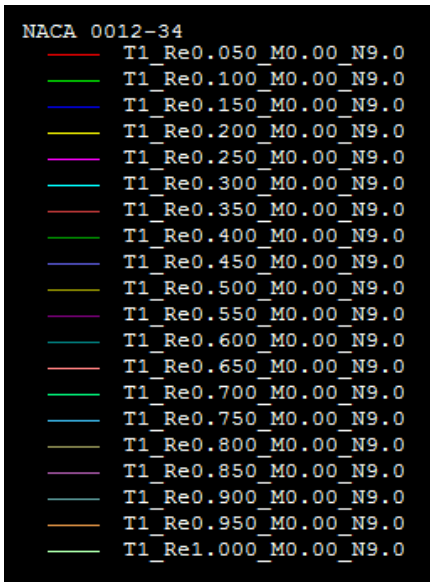


Figure 18: XFLR5 Reynolds Number Legend (NACA0012)

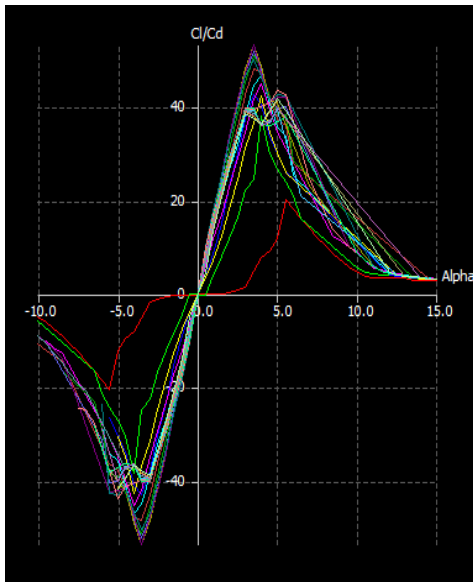


Figure 19: Lift/Drag Ratio as a Function of Angle of Attack (NACA0012)

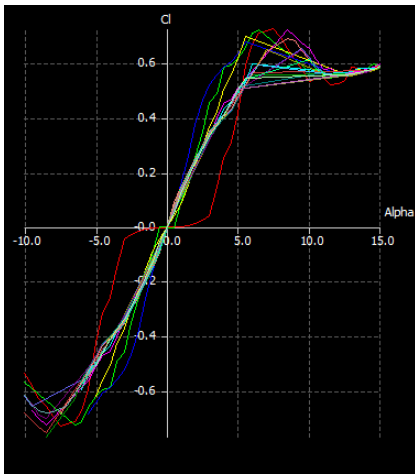


Figure 20: Lift Coefficient as a Function of Angle of Attack

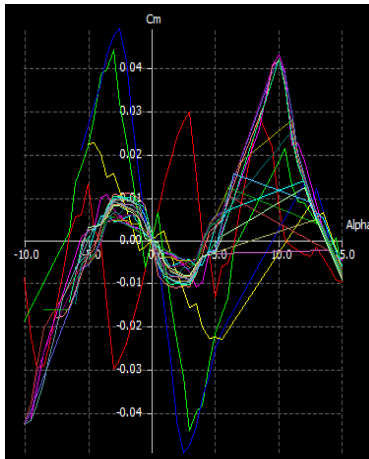


Figure 21: Moment Coefficient as a Function of Angle of Attack

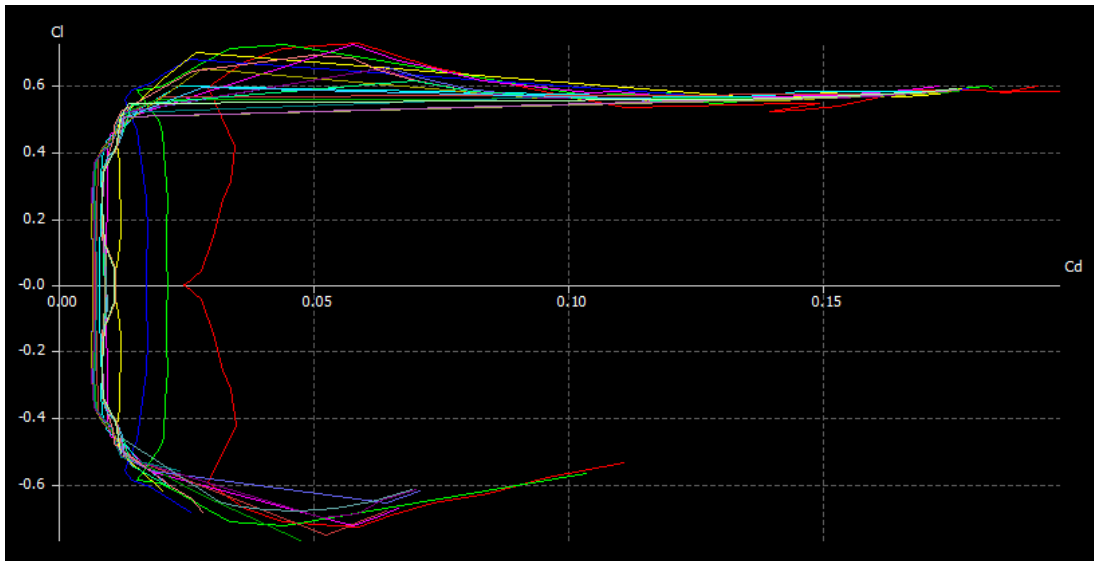


Figure 22: Lift Coefficient as a Function of Drag Coefficient for NACA 0012 Airfoil

For our horizontal and vertical stabilizers, Raymer's methods for sailplanes to size the stabilizers are used, and the results are shown in Table 6. There is no twist or taper for the vertical as well as horizontal stabilizer.

Table 6: Dimensions for stabilizers

Horizontal Stabilizer Chord Length	3.5 ft
Horizontal Stabilizer Wingspan	13.75 ft
Vertical Stabilizer Chord Length	7 ft
Vertical Stabilizer Wingspan	10 ft
Stabilator (all moving) Planform Area	25 ft ²
Rudder Planform Area	30 ft ²

Solar cells will be added to the horizontal stabilizer because there will be a negligible increase in weight, but an increase in available power, which is ideal. The setup will be similar to the wing with encapsulation and wiring going through the spar heading down to the fuselage.

12.3 DESIGN OF THE LONGITUDINAL AND DIRECTIONAL CONTROLS

For the pitch and directional control, these stabilizers will be used as combine action. The horizontal stabilizer will be a stabilator to control pitch. The stabilator will be hinged to the vertical stabilizer and will be controlled by the pilot on ground. The servos installed in the aircraft will be able to adjust the stabilator during flight, and will be able to calculate whether the aircraft is pitch up (ascending) or pitch down (descending) and adjust as necessary. The vertical stabilizer will have a rudder as shown appendix D. The servos will be connected to the flight control computer, which will be located in the fuselage, and will control the rudder and stabilator deflections.

13.0 WEIGHT AND BALANCE

13.1 COMPONENT WEIGHT BREAKDOWN

13.1.1 Maximum Power point Tracker

In order for the HALE-SPUAV to generate the greatest portion of the collected sunlight into electricity, the solar panels are usually connected to a device known as a maximum power point tracker (MPPT). The MPPT is a high efficiency DC-DC converter with an adjustable gain between the input voltage (the solar cells) and the output voltage (the batteries). In the case of the HALE-SPUAV it would be feasible to have a MPPT, which is >95% efficient: this will allow less power loss to the batteries.

MPPT controllers can be purchased for various applications; however for the purpose of this project two MPPT controllers were evaluated. The first MPPT

controller is the SunSaver MPPT Charge Controller SS-15MPPT as shown in Figure 2.3 The SunSaver MPPT is capable of working in both high and low temperature applications, with an average efficiency of 95% - 97%. The controller is design for 12V – 24V battery charging from PV array modules. The device weighs approximately 1.3 lbs, which may be too heavy since multiple units may be required for the multiple battery packs.



Figure 23: SunSaver MPPT Charge Controller SS-15

Solar Converters Inc manufactured the second MPPT controller with model number PT 12/24-3. This model (shown in Figure 24), has a nominal voltage of 12V – 24V, and a maximum output current of 3A. It also has an average efficiency of 96%. The only feature which sets this specific MPPT apart from the SunSaver is the overall weight; the Solar Converters MPPT only weighs approximately 0.3 lbs. Since multiple MPPT converters may be needed, it would be feasible to select one with a lower overall weight; which meets our performance characteristics.



Figure 24: Solar Converters Inc MPPT

13.1.2 Avionics

The autopilot has four servo channels, two 16 channel, 12 bit analog-to-digital converters, four serial ports, and five analog inputs. On-board sensors include three-axis rate gyros with a range of 300 degrees per second, three axis accelerometers with range of two *gs*, an absolute pressure sensor capable of measuring altitude to within eight feet, a differential pressure sensor capable of measuring airspeed to within 0.36 feet per second, and a standard GPS receiver. The autopilot package weighs 4.140625 lbs including the GPS antenna. The size of the autopilot is roughly 3.5 inches by 2 inches.

13.1.3 Motors

The aircraft shall contain 16 electric brushless motors (eight on each wing); the motors shall output approximately 5 KW of power. Selection of an electric motor is critical due to the weight limitations. The motor, which was selected, is the Mars Electric LLC PMAC motor (shown in Figure 25); the specifications of the motor as described in Table 7 below.

Table 7: Mars Electric LLC PMAC Motor Specs

Power	~4.5 KW Continuous → ~11 KW Peak
Voltage	24 – 48 VDC
Motor Diameter	8.00"
Shaft Size	7/8" x 1-3/4"
Key Size	3/16"
Weight	22 lbs
Efficiency	90%

The major reason in which this particular electric motor was chosen was due to its performance and the weight. The electric motor has a low enough weight and high enough performance to benefit the power requirements of the aircraft while not causing the overall weight to spike (relatively).



Figure 25: Mars Electric LLC PMAC Motor

13.2 CENTER OF GRAVITY CALCULATION

Now that the aircraft is properly sized, it will be identified where each component go. Most of the batteries, solar cells, and propulsion group will be installed onto the wing. It will help to keep wings less dihedral, which is most important with such a long wingspan. NASA Helios is an example of such damage. The payload will be located at the quarter chord of the. The airframe will primarily include the empennage and fuselage weights, and will increase from our initial estimates because of the high aspect ratio. Figure 21 shows the distribution of weights and the locations of where the center of gravity would be located. Some of the batteries would be located in the tip of the fuselage to get an aircraft center of gravity to be aft of the quarter chord of the wing. The results of the hand calculations are shown in Table 8 and figure 26.

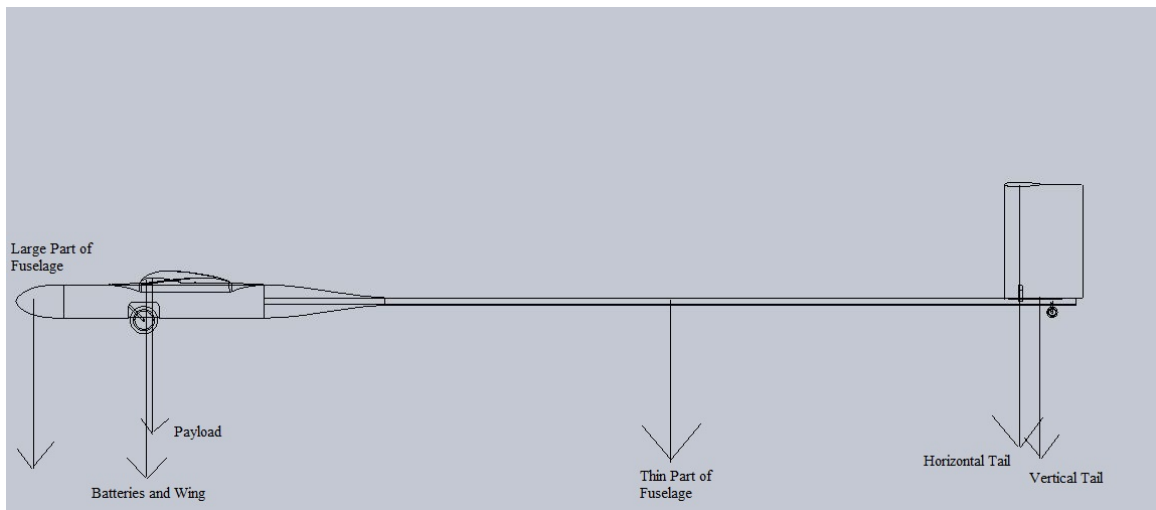


Figure 26: Aircraft CG Locations

Table 8: Component Center of Gravity

Component	X_{cg} (relative to tip of fuselage in ft)
Payload	14.472
Batteries in Wing	13.5
Large Part of Fuselage (includes some batteries)	2
Thin Part of Fuselage	64.335
Vertical Tail	92
Horizontal Tail	90.25
TOTAL	13.92

As shown in figure, the aircraft C.G. is at 14.46ft from the tip of the fuselage and the quarter chord location of the wing is located at 14.427ft which means the C.G. is located aft of the quarter chord by 0.01 ft and thus provides a static longitudinal stability to the aircraft. . For this analysis, we assumed that the aerodynamic center of the wing and aircraft is located at the quarter chord point even though the wing is cambered.

14.0 STABILITY ANALYSIS

Since the aircraft has a very large aspect ratio compare to conventional aircraft, there is possibility of wing bending and that might disturb the mission. Figure 27 shows the Nastran model of aircraft and Figure 28 is showing the wing elongation due to the vertical load. Since the total vertical displacement is not more then 5ft, the wings natural dihedral will balance it out.

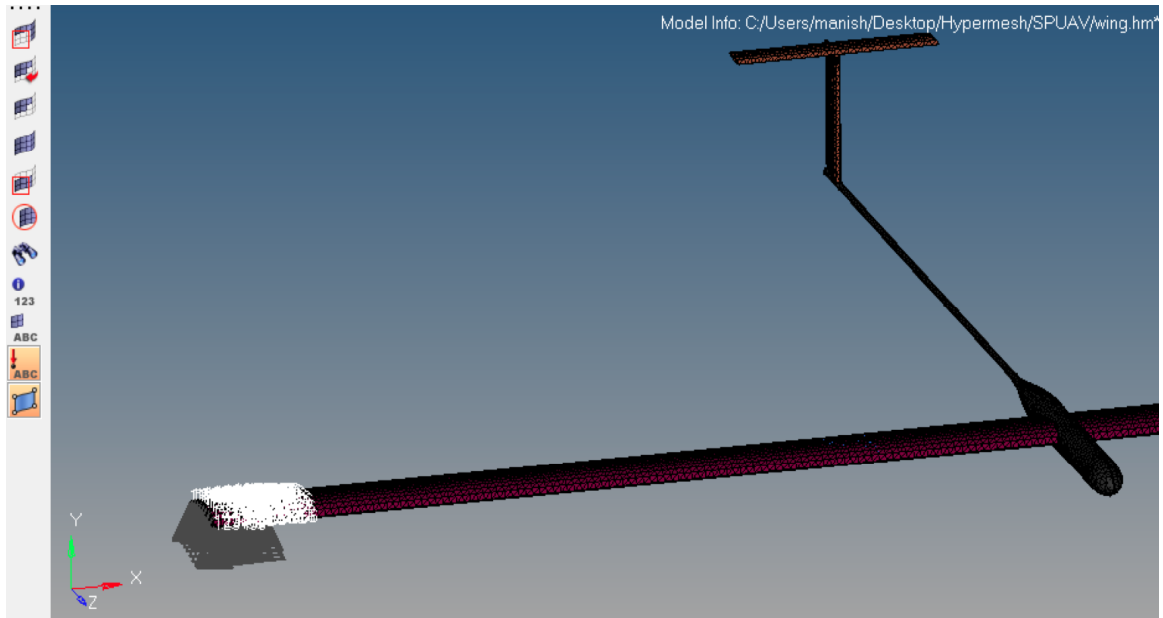


Figure 27: Nastran Model to study vertical load

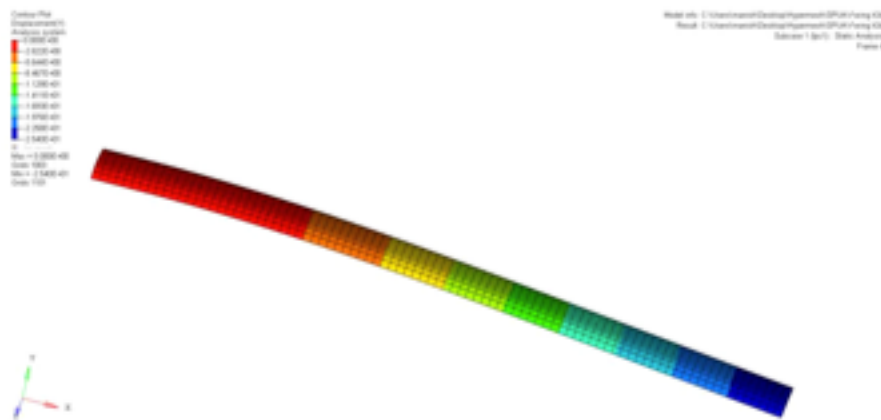


Figure 28: Vertical displacement of the Wing due to battery load

Another key component for this aircraft stability is the static margin, which is the distance between the center of gravity and the neutral point of the aircraft. The neutral point is the position of the center of gravity at which stability is neutral.

The main variables that affect the neutral point are the horizontal stabilizer area and the moment area of the horizontal about the aerodynamic center. Using Desktop Aeronautics software, the static margin can be defined as (14.1).

$$s.m. = -\frac{x_{c.g.}}{\bar{c}} + \frac{l_h S_h}{\bar{c} S_w} \frac{C_{L_{\alpha h}}}{C_{L_{\alpha w}}} - \frac{1}{C_{L_{\alpha w}}} \frac{\partial C_{m_{c.g. body}}}{\partial \alpha} \quad (14.1)$$

Table 9 shows the values for our aircraft that are specific to the static margin, as well as what each variable means.

Table 9: Static Margin Variables and Definitions

$x_{c.g.}$ (distance from wing aerodynamic center back to the c.g)	14.472 ft – 13.92 ft = 0.55 ft
C (reference chord)	8.12 ft
l_h (distance from c.g. back to tail a.c.)	91.4 ft – 13.9 ft = 76.5 ft
S_h (horizontal tail reference area)	24.08 ft ²
S_w (wing reference area)	610 ft ²
$C_{L_{\alpha h}}$ (tail lift curve slope)	~0.1
$C_{L_{\alpha w}}$ (wing lift curve slope)	~0.11
$dC_{m_{c.g. body}}/d\alpha$ (body c.g. moment coefficient curve slope)	~ -0.06

Figure 29 shows the NACA 0012 lift coefficient with the function of angle of attack. The tail lift curve slope can be found out with this figure:



The wing lift curve slope can be determined in similar manner with the use of Figure 30.

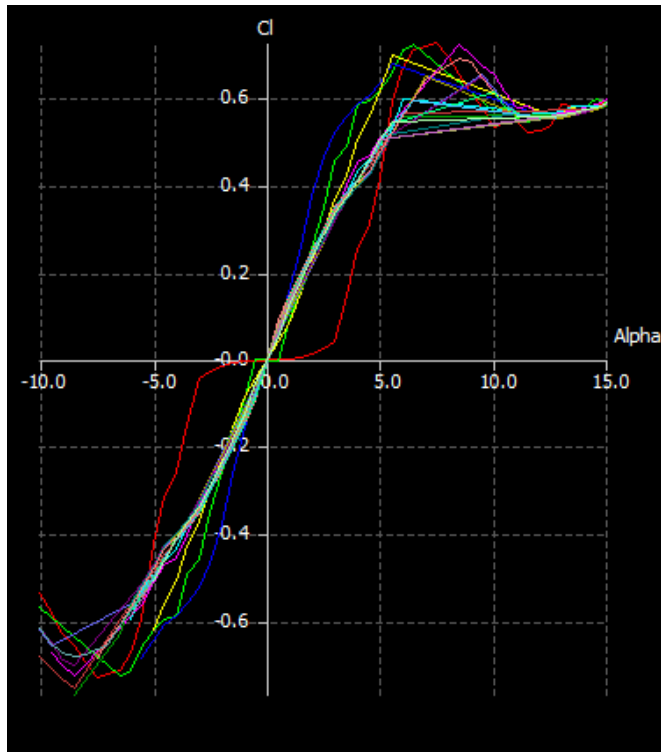


Figure 29: Lift Coefficient as a Function of Angle of Attack for NACA 0012 Airfoil

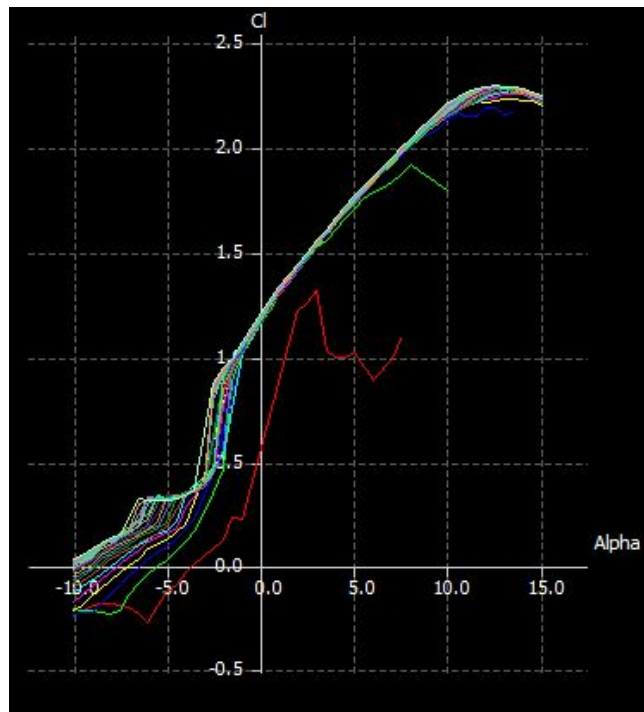


Figure 30: Lift Coefficient as a Function of Angle of Attack for Selig 1223 Airfoil

It can be calculated that the wing lift curve slope is about 0.11 same as above.

The final calculation that needs to be done is the body center of gravity moment coefficient curve slope. To do this calculation, XFLR5 data have been used. The aircraft model has been prepared as shown in the appendix F and it was possible to get values for the moment coefficient, lift coefficient, and drag coefficient over a wide range of angle of attack. Looking at C_m from Appendix F, we can see that the moment coefficient decreases by approximately 0.03 for every half angle of attack. Thus the body center of gravity moment coefficient curve slope is -0.06 as. Table 9 shows the values for all the variables for the calculation of static margin.

Plugging the values from Table 8 into the (14.1), it can be said that the static margin is 63.6%. This is much higher than what is typically found with most stable aircraft (5% - 40%), but this aircraft is very unconventional. It can be understand that this high value would push into designing a larger tail for the aircraft, which is recommended for a future analysis. Also, the aircraft would feel a bit slow during pitch and yaw movements. In addition, this value shows that the aircraft is stable aircraft since the center of lift is behind the center of gravity, which is ideal.

15.0 DRAG POLAR ESTIMATION

15.1 AIRPLANE ZERO LIFT DRAG

The airplane's zero drag calculation will be based on Roskam Part 2 methods of class one drag polar estimation. The total wetted area of the aircraft will be calculated using (15.1), which is a simplified equation from Roskam that is specific to this aircraft:

$$S_{wet,wing} = 2S_{wing} \left[1 + 0.25 \left(\frac{t}{c} \right) \right] \quad (15.1)$$

Knowing the maximum thickness of the Seling 1223 airfoil is 12.1%; the total wing wetted area can be calculated:

$$S_{wet,wing} = 2(610)[1 + 0.25(0.121)] = 1256.9$$

For the empennage, (14.1) will be used but specific to horizontal and vertical stabilizer area. The total empennage area when summing the horizontal and vertical tail areas is 55 ft². Since a NACA 0012 airfoil will be used for the empennage, the maximum thickness of the airfoil is 12%. The total wetted area would be:

$$S_{wet,emp} = 2(55)[1 + 0.25(0.12)] = 113.3$$

The fuselage-wetted area can be calculated using (15.2)

$$S_{wet,f} = \pi D_f I_f \left(0.5 + 0.135 \frac{I_n}{I_f} \right)^{2/3} \left(1.015 + \frac{0.3}{\lambda_f^{1.5}} \right) \quad (15.2)$$

In absence of flaps or slats, or any other areas that are needed to account for, the entire airplane's wetted area will be sum of three of these, which is 1629.2 ft². Roskam's methods will be used to calculate equivalence parasite area. Using the largest skin friction coefficient of 0.01 from Roskam, the equivalent parasite area

using the calculated wetted area is 16.29ft². The clean zero-lift drag coefficient will be:

$$C_{D_0} = \frac{f}{S_{wet,net}} = 0.01.$$

15.2 AIRPLANE DRAG POLAR

The drag polar will now be calculated for the airplane itself. Using the value of the calculated zero-lift drag coefficient, the overall aircraft drag coefficient can be calculated using (15.3)

$$C_D = C_{D_0} + \frac{C_L^2}{\pi e AR} \quad (15.3)$$

Assuming a lift coefficient of 1.2169 from Section 8.3, as well as an Oswald efficient factor of 0.9, the total aircraft drag coefficient can be found as 0.0231.

This will be used to find lift to drag ratio as shown:

$$\frac{C_L}{C_D} = \frac{1.2}{0.0231} = 52.01$$

XFLR5 program also used to find out lift to drag ratio for this airplane and the data are shown in appendix F. During the analysis, three different values of drag coefficient have come out hence the lift to drag ratios. Table 9 below shows all of them.

Table 9: Drag Polar Comparison

	Section 8.3	Section 15.2	XFLR5
C _L	1.2	1.2	1.2169
C _D	0.0301	0.0231	0.0321
C _L /C _D	42.09	52.01	38.4

15.3 DISCUSSION

The drag polar explains in table 9 shows that lift to drag ratio ranges from 38 to 52. The major difference is in section 15.2 analysis because other two have less difference. The 15.2 analysis does not include fuselage drag coefficient as other so that analysis should be most inaccurate among others. The average value between these two approaches can be used in further analysis if needed.

16.0 ENVIRONMENTAL/ECONOMICAL TRADEOFFS

16.1 ENVIRONMENTAL CONSIDERATION

The environmental issues that are related to HALE-SPUAV are few when compared to a commercial aircraft or model aircraft that uses fuel. However, there are still few things to consider. First, the battery and the other material are toxic and are harmful to the environment if the aircraft crashed suddenly or crashed into the sea. If the aircraft and all materials are not disposed of properly, this could harm the environment. Another issue is the fact that our aircraft is a zero fuel emission aircraft, which means that no gasoline or other oil-based fuel, like bio-fuels, is used. Fuel emission releases carbon dioxide into the atmosphere and increases the chlorofluorocarbons. That will then increases the green house effect and rest is all know. Thus it is important to reduce the carbon emission to preserve the environment.

With the invention and popularity of the hybrid vehicles, this has greatly reduced the emission from motor vehicles. However, green propulsion yet to gain enough popularity in our world. In regard to aircrafts specifically, an idea of zero

emission aircraft is still not considered since they still need significant advances in technology. Bio-fuels for commercial aircraft have been gaining some popularity, and hydrogen fuel cells are being looked at for the aircraft, but both of these still use some sort of limited energy. Solar energy not only is free of emission, but also uses sun power directly.

16.2 ECONOMIC FEASIBILITY

The increase in fuel cost over the last few years drives an alternative source of the energy, whether it is bio-fuels, hydrogen fuel cells, or solar cells. Bio-fuel has the advantage currently because aviation companies put more funding in the technology than any other alternative source of energy. The other reason bio-fuels were chosen is because it would be simple to implement them into the current commercial aircraft, which would save money since new aircraft would not have to be built. However, they are the most expensive over the time when compared to hydrogen fuel cells or solar cells because commercial aircraft will use millions of pounds of this fuel over next 50 years or so. There will come a point in time where it would be cheaper to build entirely new aircraft with solar technology than to use bio-fuel. Therefore not only will solar technology be better for the environment, but it will also be more cost-effective over a long period of time when compared to current commercial aircraft fuel.

17.0 CONCLUSION / RECOMMENDATION

With the current desire for a greener society, an alternative source of energy for aircraft is needed. There are many alternative energy solutions that are promising; including bio-fuel and hydrogen fuel cells, but nothing is as limitless as solar technology. As mentioned throughout the project, the application of high altitude long endurance UAVs can potentially be very large, whether it is in weather surveillance, studying natural disaster, or fire direction. The solar power UAV design discussed weighs 1135lb, has a large wingspan of 224ft, and holds up to 100lb of payload, which is more than enough for all the surveillance and autopilot instruments. The advances in solar technology have made it so the concept of solar powered UAVs and MAVs is not just a theory anymore. Solar power airplanes are necessary for a greener society and can be an important part of the future of aviation.

REFERENCE

1. Wikipedia, (2011). *History of solar aircrafts*, Retrieved on 01/21/2011 from:
<http://www.wikipedia.org/>
2. Boucher, R. J., "History of Solar Flight", *20th Joint Propulsion Conference*, Cincinnati, Ohio, June 11-13, 1984, AIAA-84-1429
3. NASA Facts, "Solar Powered Research", *Dryden Flight Research Center*, Edwards, California 93523
4. Bowman, W. J., Roberts, C., and Vaughan, M., "Development of a Solar Powered Micro Air Vehicle", *40th AIAA Aerospace Sciences Meeting and Exhibit*, Reno, Nevada, January 2002, AIAA-2002-0703
5. Berger, B., "NASA Studies Options Following Loss of Helios Vehicle", *Space News*, July 14, 2003,
http://www.space.com/spacenews/archive03/nasaarch_071403.html
6. AC Propulsion, "AC Propulsion's Solar Electric Powered SoLong UAV", 2004,
http://www.acpropulsion.com/ACP_PDFs/ACP_SoLong_UAV_48hr_Flight_2005-06-05.pdf
7. D.P. Raymer, *Aircraft Design: A Conceptual Approach*. 2nd Ed., AIAA Education Series, 1992.
8. J. Roskam, *Aircraft Design parts 1-8*. Roskam Aviation and Engineering Corporation, Route 4, Box 274, Ottawa, Kansas, 1985-1990.

9. Noth, A. (2008), Design of Solar Powered Airplanes for Continuous Flight (Doctoral dissertation, ETH Zürich, 2008), ETH Zürich, Sept. 2008.
10. Honsberg & Bowden, (2010). *PVCDROM. Section 2.22: Calculation of Solar Insolation*. Retrieved 11/12/2010 from.
<http://pvcdrom.pveducation.org/index.html>
11. SunPower, (2003). *SunPower Announces World's Most Efficient, Low-Cost Silicon Solar Cell*. Retrieved 11/12/2010 from http://www.ingenius.net/site/zones/greentechZONE/product_reviews/grnp_060203

APPENDICES

APPENDIX A: COMPLETE DESIGN PARAMETERS FOR SIMILAR AIRCRAFT

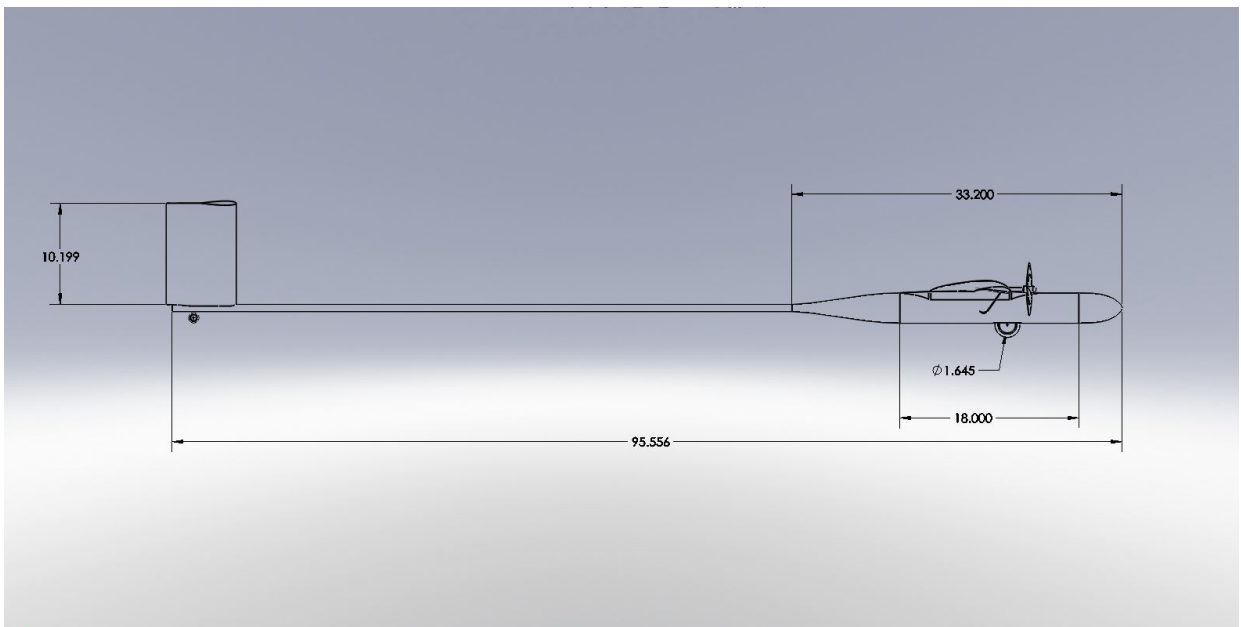
UAV	Sunrise (1974)	Solar challenger (1981)	Pathfinder plus (1988)	Centurion (1997)
Weight (lb)	27	200	700	1900
Wingspan (ft)	32	47	121	206
Cruise speed (mph)		32	20	15-18
Max power (KW)	12	8.8	12.5	31
Ceiling (ft)	8000(projected 28000)	14,300	80,201	100,000 projected
Endurance			14-15 hrs	15-16hrs
Payload (lb)			150	100-600
Propulsion type	Li-ion poly battery	Li-polymer battery	Li-polymer battry	Lithium battery and fuel cells
Construction	Spruce and balsa with maple doublers at attachment points	Nomex honeycomb wrapped round fuselage boom and wing spar	Carbon fiber, Nomex, Kevlar, plastic sheeting and plastic foam	Carbon fiber and graphite epoxy composite structure, Kevlar™, Styrofoam leading edge, plastic film covering
Comment	Failed after 28 attempts	Second prototype of Gossamer penguin. First to fly 163 miles.	record altitude, first used for environmental monitoring	The Centurion (revised from centurion) will be designed to remain aloft above 60,000 feet altitude for at least four days and nights, meeting an ERAST Level I milestone and SP/AV-HALE

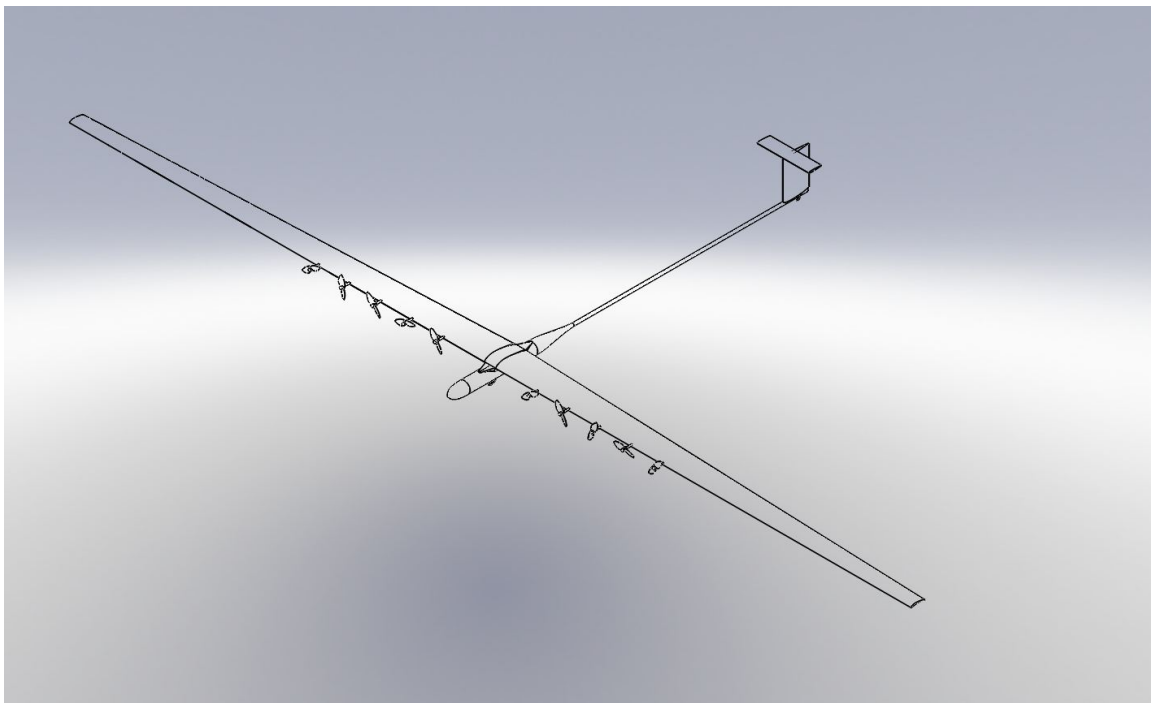
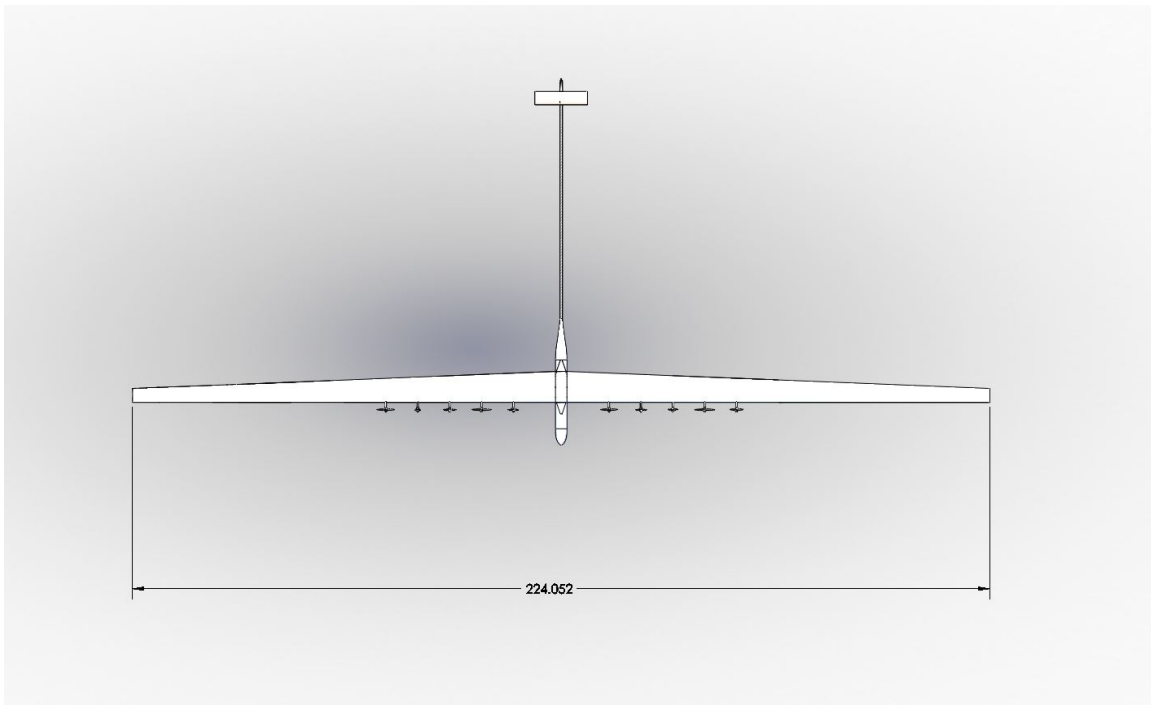
UAV	Helios HPO3 (2001)	Solar impulse (2009)	Zephyr (2010)	Sky sailor (2006)
Weight (lb)	2320	3500	117	12
Wingspan (ft)	247	208	74	11
Cruise speed (mph)	19-27	43		90
Max power (KW)	31	30		
Ceiling (ft)	96,863	39,000	70,000	1640
Endurance	24hrs	36hrs (projected)	336 hrs 22 min	
Payload (lb)	726		5	
Battery type	Lithium battery and fuel cells	Li-ion battery	Li-sulphur	Li-pool battery
Construction	Carbon fiber composite structure, Kevlar®, Styrofoam leading edge, transparent plastic film wing covering	Customized carbon fiber honeycomb sandwich structure		
Comment	Max aspect ratio wing-30.9	Manned aircraft, The team hopes that a round-the-world flight will be possible in 2012	Hand launch, max energy density >300 w-hr/kg	The vision to send to Mars an airplane that could achieve various scientific missions

APPENDIX B: LANDING GEAR POSITIONS

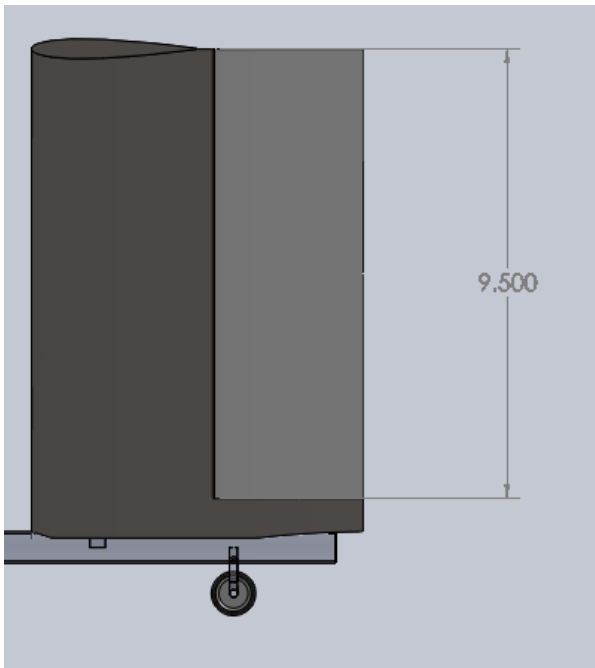
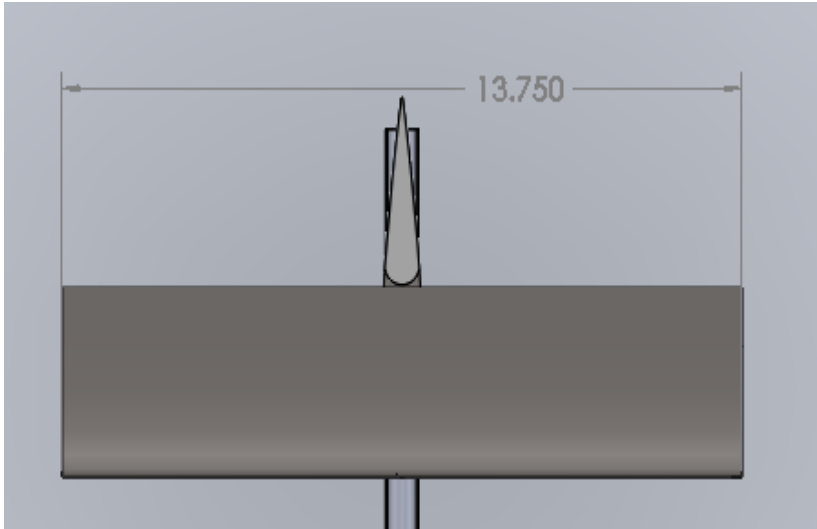


APPENDIX C & E: WING & AIRCRAFT CAD DRAWINGS





APPENDIX D: EMPENNAGE CAD DRAWINGS



APPENDIX F: XFLR5 DATA

XFLR5 v6 Beta

Wing name: Plane Name

Wing polar name: T2-3400.000 lb-Panel-VLM2-x0.000ft2

Freestream speed: 22.369 mph

Alpha	CL	ICd	PCd	TCd	CY	Cm
-5	0.687589	0.004932	0.030348	0.03528	0	-0.285939
-4.5	0.740929	0.005596	0.026885	0.032481	0	-0.317052
-4	0.794197	0.006319	0.023388	0.029707	0	-0.348432
-3.5	0.847388	0.0071	0.019963	0.027063	0	-0.380048
-3	0.900494	0.007938	0.017775	0.025713	0	-0.411631
-2.5	0.953507	0.008834	0.016713	0.025546	0	-0.443199
-2	1.006422	0.009786	0.016424	0.02621	0	-0.47483
-1.5	1.05923	0.010795	0.016173	0.026968	0	-0.506693
-1	1.111925	0.01186	0.016084	0.027944	0	-0.538749
-0.5	1.164499	0.01298	0.016042	0.029022	0	-0.571014
0	1.216946	0.014156	0.016068	0.030223	0	-0.603471
0.5	1.26926	0.015385	0.01625	0.031635	0	-0.636095
1	1.321432	0.016668	0.0166	0.033268	0	-0.668869
1.5	1.373456	0.018004	0.017024	0.035028	0	-0.701805
2	1.425326	0.019392	0.017476	0.036868	0	-0.734907
2.5	1.477035	0.020832	0.017965	0.038797	0	-0.768154
3	1.528575	0.022322	0.018492	0.040814	0	-0.80154
3.5	1.579941	0.023862	0.019001	0.042862	0	-0.835072
4	1.631126	0.02545	0.019509	0.04496	0	-0.868737


```
QInf = 133.0 mph
Alpha = 0.0000
CL = 1.2169
CD = 0.0301
Efficiency = 0.8750
Cl/Cd = 40.3919
GCm = -0.6035
Rolling Moment = 0.0000
Induced Moment = -0.0000
Airfoil Yawing Moment = -0.0000
XCP = 3.08 ft
```